Locomotive Crashworthiness Research

U.S. Department
of Transportation
**Federal Railroad
Administration**

Office of Research
and Development
Washington, DC 20590

Volume 1: Model Development and Validation

Research and
Special Programs
Administration
Volpe National
Transportation Systems Center
Cambridge, MA 02142-1093

DOT/FRA/ORD-95/08.1
DOT-VNTSC-FRA-95-4.1

Final Report
June 1995

REPORT DOCUMENTATION PAGE

Form Approved
OMB No. 0704-0188

1. AGENCY USE ONLY (Leave blank)	2. REPORT DATE	3. REPORT TYPE AND DATES COVERED
	June 1995	Final Report January 1994 – October 1994

4. TITLE AND SUBTITLE
Locomotive Crashworthiness Research
Volume 1: Model Development and Validation

5. FUNDING NUMBERS
R5001/RR528

6. AUTHOR(S)
Ronald A. Mayville, Richard G. Stringfellow, Robert J. Rancatore, Thomas P. Hosmer

7. PERFORMING ORGANIZATION NAME(S) AND ADDRESS(ES)
Arthur D. Little, Inc.
Acorn Park
Cambridge, MA 02140-2390

8. PERFORMING ORGANIZATION REPORT NUMBER
DOT-VNTSC-FRA-95-4.1

9. SPONSORING/MONITORING AGENCY NAME(S) AND ADDRESS(ES)
U.S. Department of Transportation
Research and Special Programs Administration
Volpe National Transportation Systems Center
Kendall Square, Cambridge, MA 02142-1093

10. SPONSORING/MONITORING AGENCY REPORT NUMBER
DOT/FRA/ORD-95/08.1

11. SUPPLEMENTARY NOTES
This research is sponsored by the Federal Railroad Administration, Office of Research and Development, Washington, DC 20590

12a. DISTRIBUTION/AVAILABILITY STATEMENT
This document is available to the public through the National Technical Information Service, Springfield, VA 22161

12b. DISTRIBUTION CODE

13. ABSTRACT (Maximum 200 words)

This report is the first of four volumes concerning a study to investigate the costs and benefits of equipping locomotives with various crashworthiness features beyond those currently specified by the Association of American Railroads S-580 specification. The study includes model development and validation, design concept generation and evaluation, and prioritization of concepts.

This first volume provides a description of the modeling efforts, including the development of structural damage (crush) and collision dynamics models using commercially available computer programs. Refinement and validation of the models was carried out through application to the conditions for three actual head-on collisions involving closing speeds ranging from 18 to 43 mph. The model is shown to provide a good simulation for these types of accidents.

14. SUBJECT TERMS
Rail Vehicle; Transportation; Safety; Locomotive Crashworthiness; Collisions; Structural Analysis, Dynamics Analysis

15. NUMBER OF PAGES
52

16. PRICE CODE

17. SECURITY CLASSIFICATION OF REPORT	18. SECURITY CLASSIFICATION OF THIS PAGE	19. SECURITY CLASSIFICATION OF ABSTRACT	20. LIMITATION OF ABSTRACT
Unclassified	Unclassified	Unclassified	Unlimited

PREFACE

In September 1992, the Congress passed Public Law 102-365, the Railroad Safety Enforcement and Review Act, which required, in part, that the Secretary of Transportation conduct research and analysis to consider the costs and benefits of several types of crashworthiness improvement features.

This report summarizes the development of computer models, and related engineering calculations, which were used to analyze the crashworthiness of the cab area in existing road freight locomotives and to provide quantitative estimates of the costs and benefits of the crashworthiness improvement features. The work was carried out by Arthur D. Little, Inc., under contract to the Volpe National Transportation Systems Center, from January 3, 1994, to March 31, 1995. The work was conducted as part of the Center's support to the Office of Research and Development, Federal Railroad Administration.

This is the first of four volumes. Volume 2 covers the representation of proposed crashworthiness features, evaluation of their effectiveness in limiting cab intrusion, and evaluation of their influence on occupant survivability. Volume 3 discusses the pros and cons, and summarizes the estimated costs versus benefits, for each of the represented crashworthiness improvement features. Volume 4 extends the modeling to additional effects, and the analysis to higher closing speeds.

During the course of the study, further work was assigned to provide for additional studies of selected freight locomotive crashworthiness improvement features in collisions at higher closing speeds and for evaluation of the crashworthiness of the cabs in control cars used in passenger service. The additional freight locomotive studies will appear as volume 4 of this series. The work on control car cabs will be published as a separate report.

METRIC/ENGLISH CONVERSION FACTORS

ENGLISH TO METRIC

LENGTH (APPROXIMATE)

1 inch (in)	=	2.5 centimeters (cm)
1 foot (ft)	=	30 centimeters (cm)
1 yard (yd)	=	0.9 meter (m)
1 mile (mi)	=	1.6 kilometers (km)

AREA (APPROXIMATE)

1 square inch (sq in, in^2)	=	6.5 square centimeters (cm^2)
1 square foot (sq ft, ft^2)	=	0.09 square meter (m^2)
1 square yard (sq yd, yd^2)	=	0.8 square meter (m^2)
1 square mile (sq mi, mi^2)	=	2.6 square kilometers (km^2)
1 acre = 0.4 hectare (he)	=	4,000 square meters (m^2)

MASS - WEIGHT (APPROXIMATE)

1 ounce (oz)	=	28 grams (gm)
1 pound (lb)	=	0.45 kilogram (kg)
1 short ton = 2,000 pounds (lb)	=	0.9 tonne (t)

VOLUME (APPROXIMATE)

1 teaspoon (tsp)	=	5 milliliters (ml)
1 tablespoon (tbsp)	=	15 milliliters (ml)
1 fluid ounce (fl oz)	=	30 milliliters (ml)
1 cup (c)	=	0.24 liter (l)
1 pint (pt)	=	0.47 liter (l)
1 quart (qt)	=	0.96 liter (l)
1 gallon (gal)	=	3.8 liters (l)
1 cubic foot (cu ft, ft^3)	=	0.03 cubic meter (m^3)
1 cubic yard (cu yd, yd^3)	=	0.76 cubic meter (m^3)

TEMPERATURE (EXACT)

[(x-32)(5/9)] °F = y °C

METRIC TO ENGLISH

LENGTH (APPROXIMATE)

1 millimeter (mm)	=	0.04 inch (in)
1 centimeter (cm)	=	0.4 inch (in)
1 meter (m)	=	3.3 feet (ft)
1 meter (m)	=	1.1 yards (yd)
1 kilometer (km)	=	0.6 mile (mi)

AREA (APPROXIMATE)

1 square centimeter (cm^2)	=	0.16 square inch (sq in, in^2)
1 square meter (m^2)	=	1.2 square yards (sq yd, yd^2)
1 square kilometer (km^2)	=	0.4 square mile (sq mi, mi^2)
10,000 square meters (m^2)	=	1 hectare (ha) = 2.5 acres

MASS - WEIGHT (APPROXIMATE)

1 gram (gm)	=	0.036 ounce (oz)
1 kilogram (kg)	=	2.2 pounds (lb)
1 tonne (t)	=	1,000 kilograms (kg)
	=	1.1 short tons

VOLUME (APPROXIMATE)

1 milliliter (ml)	=	0.03 fluid ounce (fl oz)
1 liter (l)	=	2.1 pints (pt)
1 liter (l)	=	1.06 quarts (qt)
1 liter (l)	=	0.26 gallon (gal)
1 cubic meter (m^3)	=	36 cubic feet (cu ft, ft^3)
1 cubic meter (m^3)	=	1.3 cubic yards (cu yd, yd^3)

TEMPERATURE (EXACT)

[(9/5) y + 32] °C = x °F

QUICK INCH - CENTIMETER LENGTH CONVERSION

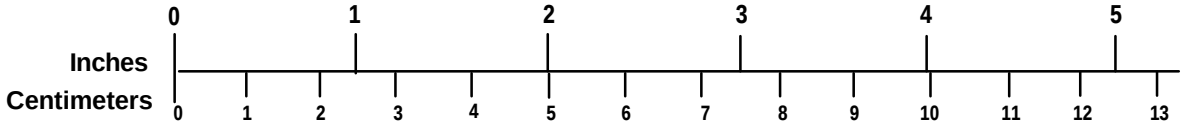

QUICK FAHRENHEIT - CELSIUS TEMPERATURE CONVERSION

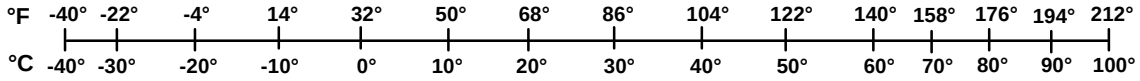

For more exact and or other conversion factors, see NIST Miscellaneous Publication 286, Units of Weights and Measures.
Price $2.50 SD Catalog No. C13 10286

Updated 6/17/98

TABLE OF CONTENTS

LIST OF FIGURES

LIST OF FIGURES (continued)

Figure **Page**

LIST OF FIGURES (continued)

LIST OF TABLES

1. INTRODUCTION

Arthur D. Little and its subcontractors, Arvin/Calspan and Parsons Brinckerhoff, conducted studies of locomotive crashworthiness in support of the Federal Railroad Administration's (FRA) response to Public Law 102-365. This law includes a statement that the Secretary of Transportation shall conduct research and analysis to consider the costs and benefits associated with equipping locomotives with the following crashworthiness features:

- Braced collision posts
- Crash refuges
- Rollover protection devices
- Uniform sill heights
- Deflection plates
- Anticlimbers
- Shatterproof windows
- Equipment to deter post-collision entry of flammable liquids

The Arthur D. Little team was awarded a contract to conduct engineering analyses to identify and evaluate various design concepts for the features described above. In particular, the team was asked to perform this evaluation with respect to the currently applied Association of American Railroads (AAR) industry standard, S-580, summarized in table 1-1. This standard applies to new road-type locomotives built after August 1, 1990.

Table 1-1. Summary of AAR's S-580 Standard on Locomotive Crashworthiness Requirements

Component	Requirement
Anticlimbers	Sustain an ultimate vertical load of 200,000 lbf at the short hood end
Collision posts	Two, each of which shall sustain an ultimate load of 200,000 lbf at 30 inches above the deck and 500,000 lbf at the deck
Short hood structure	The product of skin thickness and yield strength shall be at least 0.5 inches times 25,000 psi

The overall approach to the project included information gathering on locomotive design and crashworthiness, the development of computer models to evaluate crashworthiness, and the generation and evaluation of design concepts that could potentially improve locomotive cab survivability. No testing was included in the program. Rather, models were validated to the extent possible by comparing predicted results to actual accidents.

This report describes the locomotive collision computer models developed and validated in the project; it is the first in a series of four reports generated to describe the results of the entire project.

2. COLLISION MODES AND COMPONENT INTERACTIONS

The development of the computer models and the choice of accident types to which they should be applied have been guided by many aspects of train collisions, including the possible and likely collision modes, locomotive structural design, and considerations on how colliding locomotives interact.

2.1 COLLISION MODES

The primary types of collisions between two trains are: (1) head-on; (2) rear-end; and (3) side impact. Of these, the head-on collision appears to represent the greatest threat to the locomotive crew. Grade crossing accidents and rear-end collisions in which a lead locomotive is involved also challenge the front end but less seriously than the head-on collision. The S-580 specification, with its emphasis on front end components, is clearly directed toward protection against the head-on collision. For these reasons, we selected the head-on collision as the primary crash scenario type with which to evaluate crashworthiness design concepts (described in volume 2).

Several possible vehicle collision modes can occur when two trains collide as illustrated schematically in figure 2-1. For some of these the vehicles remain in line and on the track while for others derailment occurs. The most serious of these modes in terms of risk of injury and fatality to the cab occupants is override, since such a mode can lead to crushing of the cab. This is the mode we have examined in greatest detail, although vertical and lateral buckling as well as simple crushing have also been considered.

An examination of the approximate energy absorbed for each of the modes provides an initial basis for establishing closing speeds above which massive destruction of a lead locomotive seems likely. Table 2-1 lists examples of the estimated changes in energy for various modes that could occur in a head-on collision between two locomotives. Values are provided for a 200-ton locomotive as derived from results to be presented below. Figure 2-2 is a plot of the kinetic energy of one 200-ton locomotive as a function of closing speed in an equal speed collision. This energy is the minimum that must be converted to some other form by at least one of the locomotives if the locomotives remain approximately in line. The energy that must be converted by at least one of the locomotives is greater when more locomotives are included in each consist; the basis for this latter assertion is described in section 3.2.2.

Comparison of the approximate energy converted by different modes (table 2-1) and the kinetic energy of a single locomotive in an equal speed collision (figure 2-2) shows how difficult it is for a locomotive to sustain controlled damage in a head-on collision as closing speed increases.

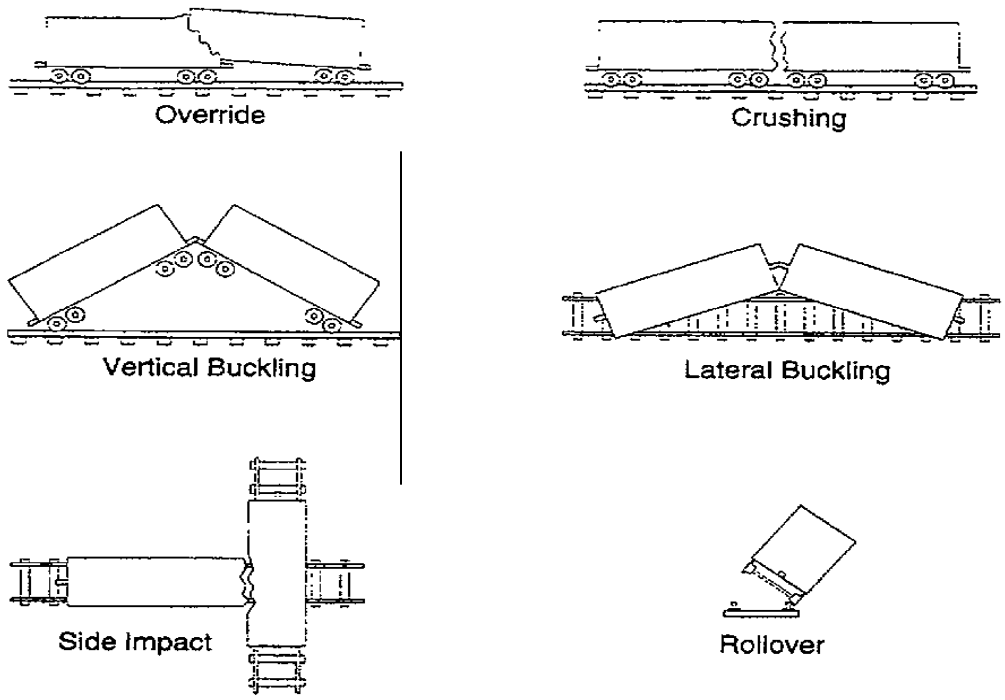

Figure 2-1. Possible Vehicle Collision Modes in Train Collisions

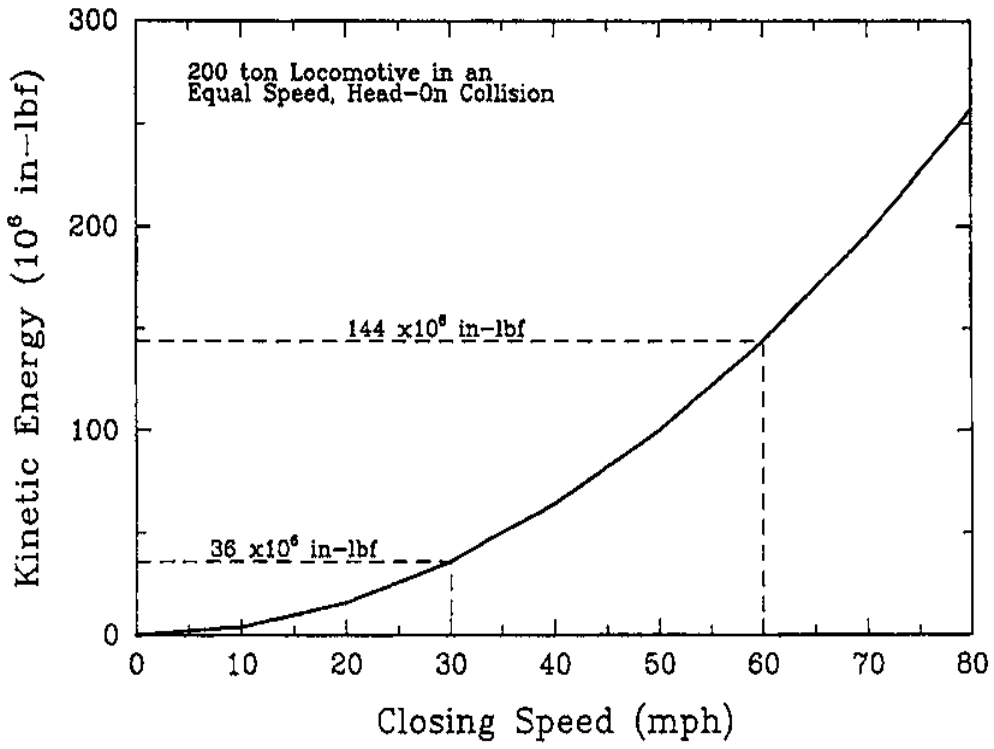

Figure 2-2. Kinetic Energy of a Single 200-Ton Locomotive as a Function of Speed

Table 2-1. Examples of Energy Converted by Different Modes in Head-On Collisions

Crash Mode	Energy Converted (10^6 in-lbf)
Crush (4 ft) of S-580 collision posts	~20
Potential energy of lifting a 200-ton locomotive end 10 ft	~20
Bending of front underframe for 1-ft longitudinal crush	~20

2.2 LOCOMOTIVE DESCRIPTION

We are most interested in the short hood end of the locomotive, since this is the usual location of engineers and the end at which most of the deformation occurs in head-on collisions. Figure 2-3 is an illustration of the short hood end of a typical freight locomotive showing the structural elements most likely to participate in a collision. The geometry of these components is important in determining the manner and order in which they will interact with the end of another locomotive and their structure and materials are important in determining their strength and load-deformation characteristics.

The underframe is the primary structural member of the locomotive. It supports the engine and other equipment and provides static and fatigue buff and draft strength. Its structure consists, in general terms, of two longitudinal webs with wide plates welded on top and bottom to form a box type structure [1]. As a result, it is very rigid and strong in tension or compression and is the structure to which the other components discussed here are attached.

The coupler is carried by the draft gear support structure, which is welded to the bottom of the underframe. The coupler projects farthest from the end of the locomotive and in its extreme buff, or compressed, state bears against the striker plate of the draft gear support structure, which is also very stiff. In a head-on collision, the coupler and the draft gear support structure will be the first components loaded.

The anticlimber projects horizontally about two to four inches less than the projection of the coupler in its buff position. The top of the anticlimber is level with the top walking surface of the underframe. The underside of the anticlimber on S-580 locomotives generally includes several significant web or support plates angled down to the bottom plate of the underframe structure; these plates provide the primary vertical load carrying capacity. At least two of the angled web plates are in line with the primary web plates of the underframe.

The collision posts are relatively thick plates, welded adjacent to or directly onto the primary longitudinal webs of the underframe. They are enclosed in and, in S-580 locomotives, welded to the short hood structure, and they project above the floor of the cab by different amounts depending on the locomotive model.

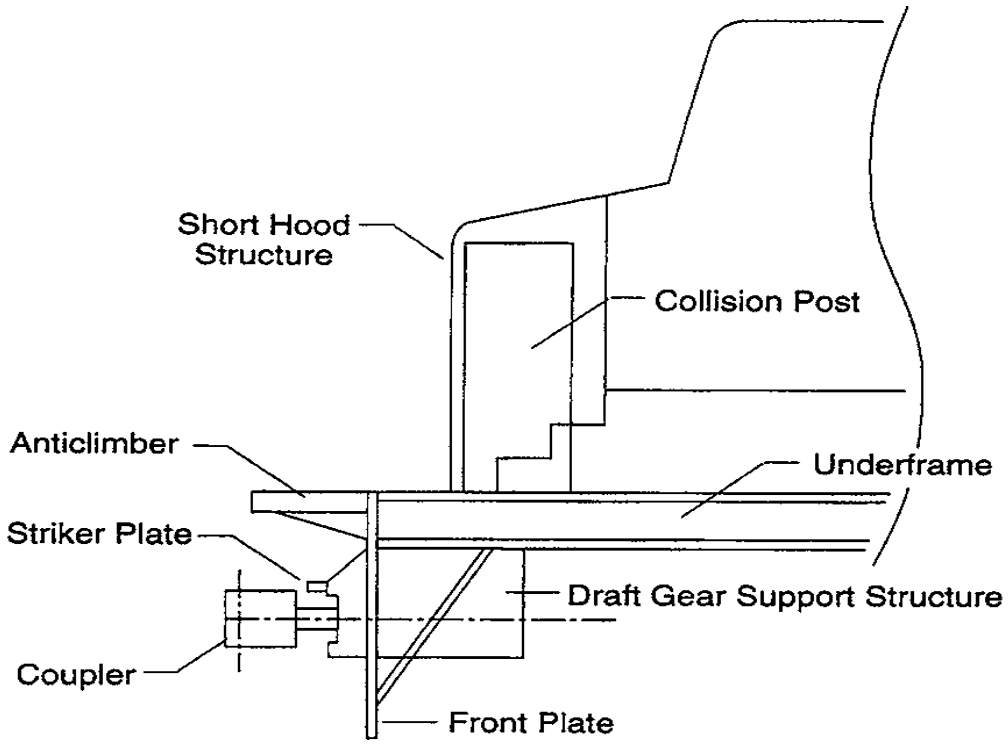

Figure 2-3. Illustration of a Road Freight Locomotive Front End

The short hood is a shell that forms the housing of various cab components. Its nose projects as much as two feet in front of the collision posts.

Standard structural materials are generally used for the locomotive components described above. These include materials similar to ASTM A36, AISI 1020, and ASTM A572, or other low alloy steels. Minimum yield strengths range from 30 to 100 ksi.

2.3 LOCOMOTIVE FRONT END INTERACTIONS

It has been very important in the development of the computer models to envision how two locomotives colliding head-on will interact. In particular, we are concerned with interactions that result in override; this mode can possibly lead to crushing of the cab if the collision posts are overloaded. We separate the phenomenon of override into two steps: override initiation and total override. Total override corresponds to one underframe riding on top of another underframe. In our model, we artificially induce override initiation and allow it to follow a particular interaction sequence to determine whether total override will occur (see section 3.2.1).

Figure 2-4 illustrates the two sequences of total override we have considered. In each of these, we assume that there is some loading of the couplers and the draft gear support structure and that override is initiated by ramping between either the anticlimbers or the couplers. What happens next depends on whether and in what order the draft gear support structures fail.

In the first interaction sequence, the draft gear support structure of the initially overriding locomotive fails, permitting total override to occur. Such a sequence can occur if the coupler of the overriding locomotive fails during initial impact or bears against the underframe, which is considerably stronger. In fact, it appears that two of the accidents used for model validation, including one in which a locomotive satisfying S-580 was overridden, follow this sequence.

In the second interaction sequence, the draft gear support structure of the initially overridden locomotive fails before that of the overriding locomotive. In this case, the anticlimber of the overridden locomotive becomes "trapped" between the anticlimber and the draft gear support structure of the overriding locomotive. This sequence can absorb substantially more energy than the first because it leads to some interaction of the underframes. We expect that total override will occur when the draft gear support structure of the overriding locomotive fails, for example, by vertical loads induced by the collision.

The first sequence is the one for which the collision model has been designed. Accident data, presented below, show that this sequence occurs and, because it absorbs less energy than the second sequence, it provides a more rational baseline for assessing the various design concepts.

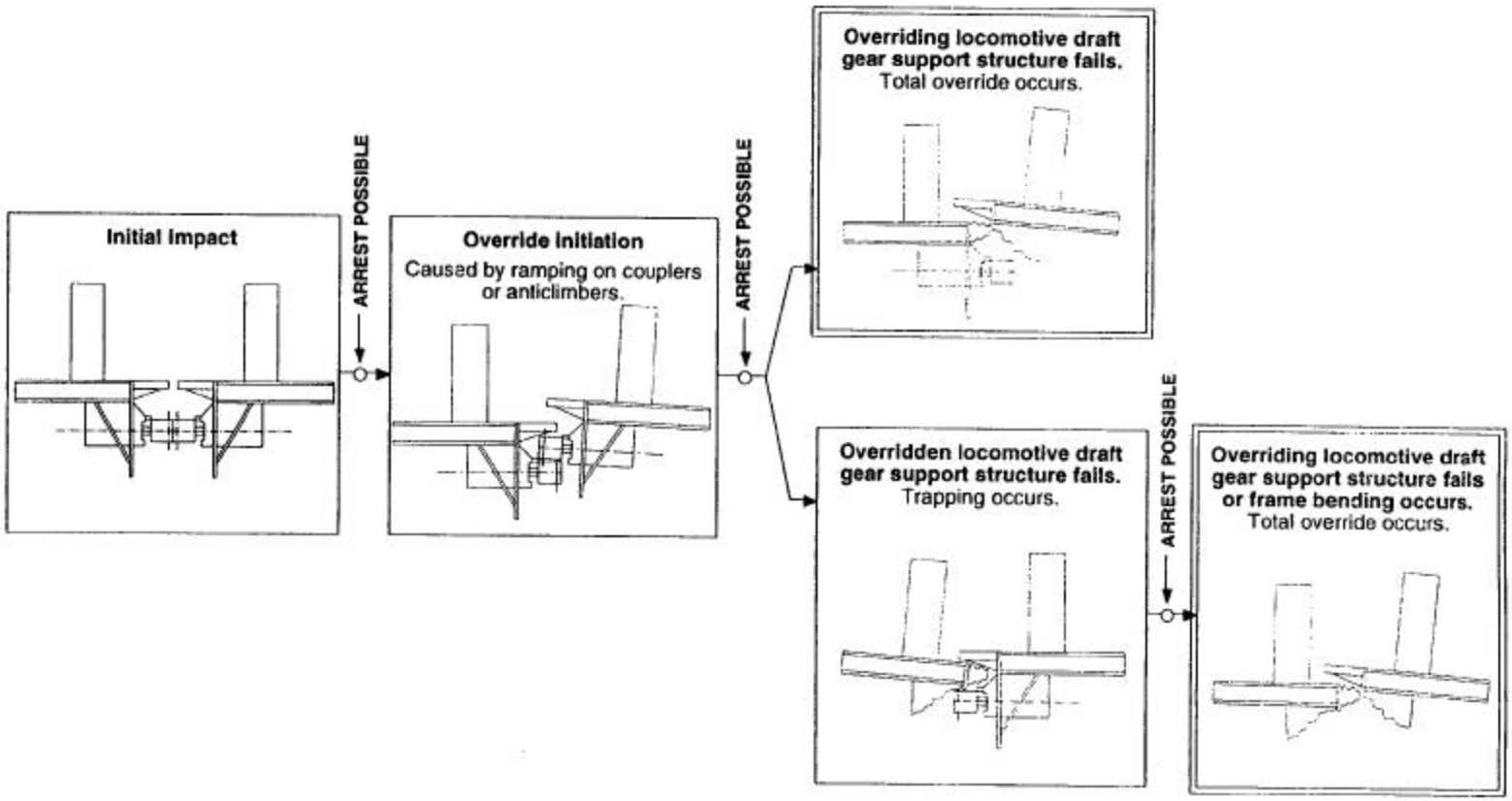

Figure 2-4. Two Potential Head-On Collision Override Sequences

3. MODEL DESCRIPTIONS

3.1 OVERVIEW

There are three elements to the computer modeling, the most important of which is the collision dynamics model, which is used to determine consist trajectories, amount of crush experienced by the cab, and the cab crash pulse, that is, the acceleration-time history to which the occupants could be subjected. The collision dynamics model is a lumped mass parameter system that provides a relatively simple description of the locomotive and consist. This approach is similar to that taken in previous studies (for example, reference [2]). The other elements of the overall model are: the structural damage model, which is used to calculate the load-deformation characteristics of various locomotive components used as input to the collision dynamics model; and the occupant survivability model, which utilizes the crash pulse to estimate the loads likely to be experienced by the cab occupant. The structure of the model is illustrated in figure 3-1. The occupant survivability model is described in volume 2.

The collision dynamics model is a lumped mass parameter system that provides a relatively simple description of the locomotive and consist. Vehicle body and trucks are each represented by a single mass and the end components are represented by geometrically simple beam elements. The complex crushing behavior of the components is incorporated by assigning to the beam elements nonlinear load-deformation curves that have been derived from detailed elastic-plastic finite element analyses.

Three actual train accidents were used to guide development and validation of the computer models. These accidents, which we refer to here as the crash scenarios, were taken from FRA reports. They consist of three head-on collisions at three different closing speeds.

3.2 COLLISION DYNAMICS MODEL

The collision dynamics model provides the primary outputs for making the occupant survivability assessment. These are the crash pulse - accelerations vs. time - and the degree of cab crushing. The model consists of lumped masses with longitudinal extensions whose characteristics are nonlinear and determined from the structural damage model described in section 3.3 below. The particular model developed here is designed to treat only in-line collisions corresponding to the crash scenarios; rollover and side impact are not treated. In fact, motion is restricted to a vertical plane that includes the original longitudinal line of the consist. The manner in which lateral buckling is treated is discussed below.

The computer program ADAMS, version 7.0, was used to construct the collision dynamics model. ADAMS is a multibody systems analysis program [3]. The description of the model is divided into two sections for clarity: front end interaction and multiple vehicle consist dynamics.

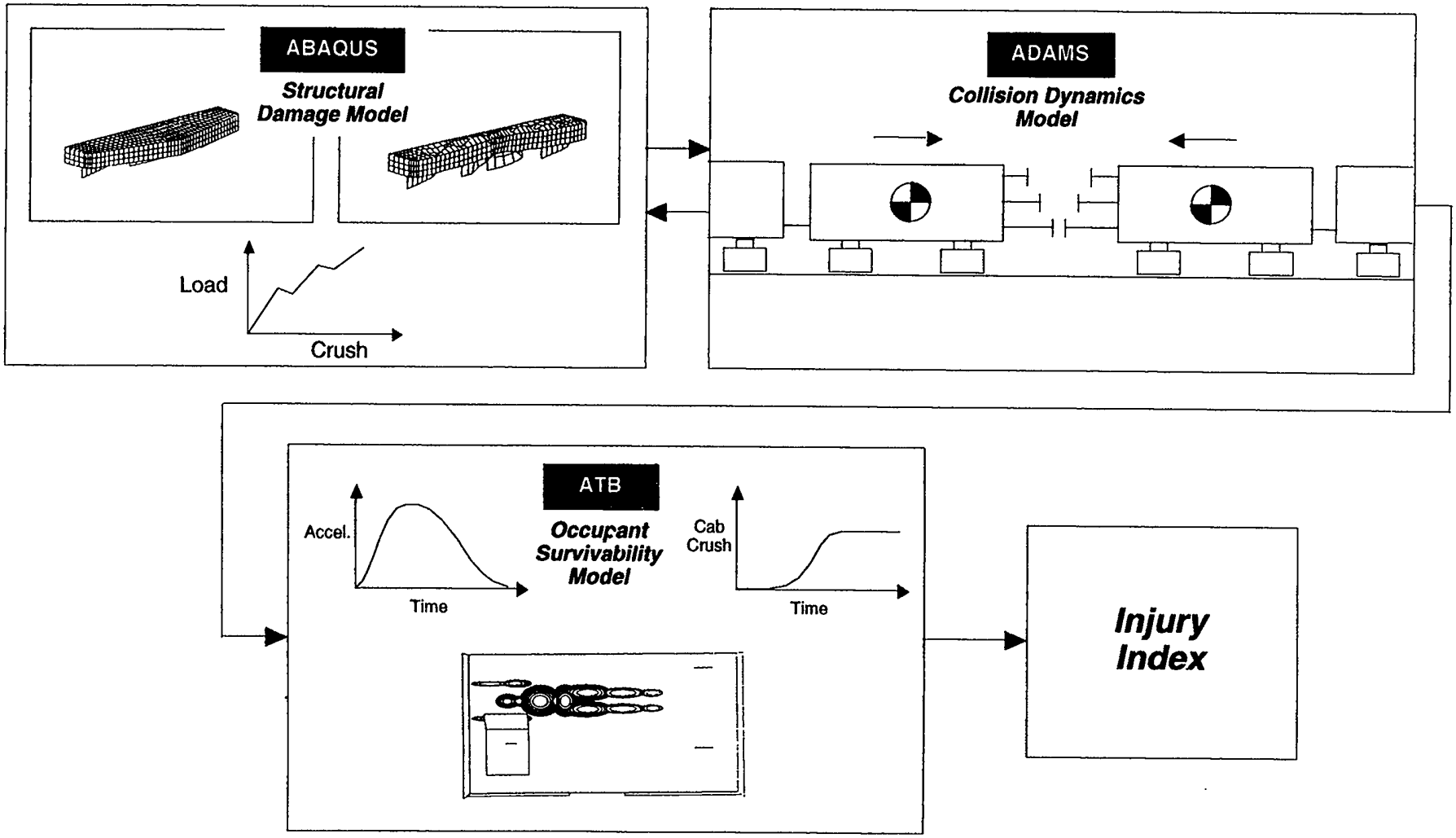

Figure 3-1. Overview of the Crashworthiness Modeling Approach

3.2.1 Front End Interaction Model

Figure 3-2 illustrates the geometric model used for the front locomotives in the collision scenarios. It consists of three masses: one for the locomotive body and two for the trucks. Only the locomotive mass possesses rotational inertia; the trucks are constrained to follow a horizontal line corresponding to the rails. There are vertical and horizontal springs between the locomotive body and the trucks and a vertical damper between each truck and the body. The vertical truck spring stiffness increases by a factor of 100 after a certain downward deflection, representing a hard stop, and the springs provide no force after a certain upward deflection, representing lift-off at the bolster. Braking friction is simulated between the trucks and ground to be constant at all times, reflecting a constant, non-skid emergency braking action.

The front end of the locomotive includes three impact elements to represent the crushing response of front-end structural components (figure 3-3). These are: (1) the coupler hardware and draft gear support structure; (2) the anticlimber and underframe; and (3) the short hood and collision posts.

Each of the impact elements has some common features. The element itself is rigid and permitted to translate only in the horizontal direction (relative to the locomotive body). Load is transmitted from an element to the locomotive body only when the tip or surface of the element is within a small prescribed distance of a point or surface on the opposing locomotive. The elements transmit vertical and longitudinal loads and, when relative sliding occurs, tangential friction loads. The longitudinal crush behavior of an element follows the relevant curve determined from the structural damage model, described below. Crush is irreversible and, if there is unloading, the previous maximum load must be exceeded for additional crush to occur. Vertical crush is not currently modeled; however, the model checks to ensure that vertical strength is not exceeded.

One of the locomotives includes a ramp at the tip of its anticlimber element (figure 3-3). This is the mechanism used to initiate the override. A ramp angle of 20 degrees to the horizontal has been used in our calculations and the length of the ramp depends on the locomotive modeled.

In a head-on collision between two locomotives the sequence of possible element interactions is as follows (compare figure 2-4). Longitudinal load is first transmitted when the tips of the coupler/draft gear support structure elements make contact. Next, the anticlimber elements carry load when their tips contact, at which time the tip of the overridden anticlimber element slides below and along the ramp of the overriding anticlimber element (figure 3-3). If the override continues, the next possible interaction is between the tip of the coupler/draft gear support structure of the overriding locomotive and the anticlimber/underframe element of the overridden locomotive; this occurs when the tip of the overriding anticlimber is in proximity to the front plate surface of the overridden locomotive. Again, if override continues, the next possible interaction occurs when the tip of the anticlimber element of the overriding locomotive contacts the tip of the short hood/collision post element.

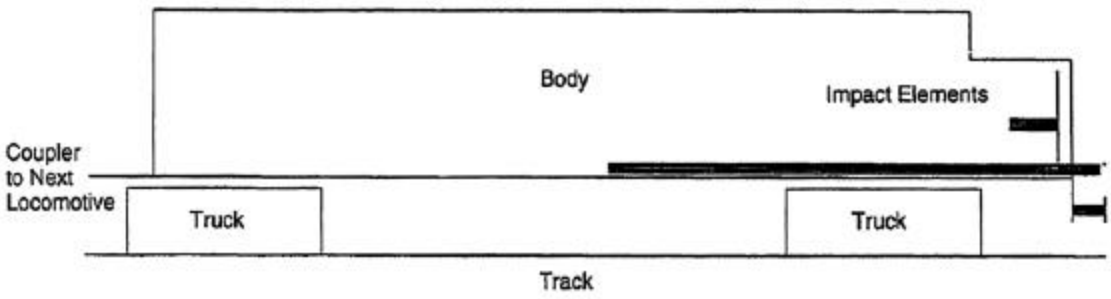

Figure 3-2. Locomotive Geometric Idealization Used in the ADAMS Model

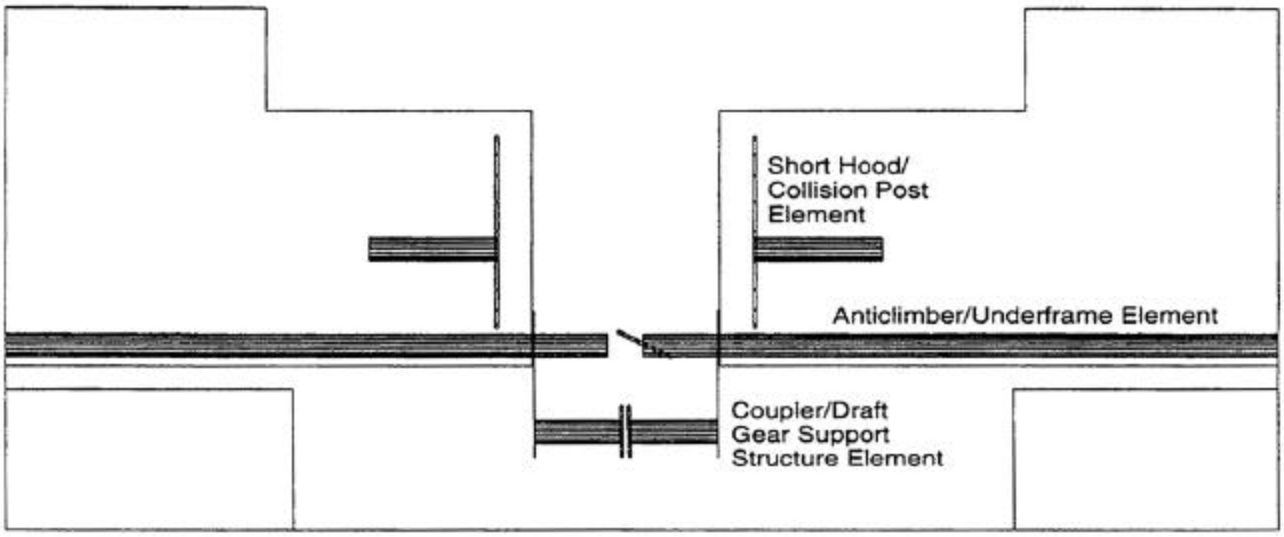

Figure 3-3. Locomotive Front End Impact Elements in ADAMS

The exact sequence and timing of contact events in the model depends on several factors, including the amounts of prior crush experienced by the elements - for example, the crush and possible failure of the overriding locomotive's coupler/draft gear support structure before interaction with the underframe - and the overall dynamics of the consists.

The baseline load-crush curves used for the three elements are presented in the section on structural damage below.

3.2.2 Multiple Vehicle Model

The multiple vehicle model must account for the effect, if any, that all vehicles have on determining the crush and acceleration behavior of the lead locomotive, in which we are most interested. It is not uncommon to have as many as five locomotives and nearly 100 other trailing vehicles in a train. We sought in our modeling efforts to determine a few important phenomena: which of the vehicles in the train must be modeled and what is the effect of trailing vehicle derailment. As presented below, our results show that when the trailing cars have lower crush strength than the locomotives a good simulation of the lead locomotive crush can be obtained by including only the locomotives. Our results also show that by the time trailing vehicles derail, the crush in the first locomotive has been determined, indicating that such derailment need not be modeled in this study. Note, however, that such trailing vehicle derailment is very important in determining the dynamics of the remaining vehicles.

3.2.2.1 The Effect of Trailing Vehicles on Crush

Our approach to assessing the number of vehicles to include in the dynamics model was based on both numerical and analytical calculations. In general, we calculated the amount of energy that was dissipated in the first vehicle, or locomotive, for various consist configurations.

A set of one-dimensional dynamic computer runs was first made, in which two consists collide at equal but opposite speeds; a speed of 15 mph (closing speed equal to 30 mph) was used here. The number of vehicles in each consist was varied to determine the effect on energy dissipation in the first vehicle. Each consist was made up of various numbers of 200-ton vehicles, representing locomotives, and 100-ton vehicles, representing trailing cars. The crush response curve for both types of vehicles had the same form but the magnitude of the crush load for the locomotives was always twice that of the trailing vehicles.

The results for analyses made with all 200-ton vehicles are shown in figure 3-4 for two types of load-crush curves. The figure shows that the energy dissipated in the first locomotive does not plateau but continues to rise with each locomotive added for both the rigid-plastic crush behavior and the, currently, more realistic peak load response. An implication of this result is that consists with fewer locomotives, a trend in the industry with the introduction of alternating current traction motor (AC) technology, will be less susceptible to damage and crush.

On the other hand, if a set of locomotives is followed by trailing cars of lower crush strength, then the energy dissipated in the first locomotive levels off quickly with additional trailing vehicles. Figure 3-5 shows an example of this for five leading locomotives. These results show that, for this case, the extra energy dissipated in the first locomotive by adding trailing vehicles does not exceed 10% of the energy dissipated without trailing vehicles.

An analytical explanation for these numerical results is presented in Appendix A but a brief description is provided here. Trailing cars have minimal effect on the crush of the first locomotive because they are only able to transmit a certain force \em\ their crush force \em\ to the locomotives before them. If there are several locomotives before the trailing vehicles, then the force they apply, and the contribution to energy dissipated, will dominate that contributed by the trailing vehicles.

Of course, the exact amount of energy that must be dissipated by deformation in the lead locomotive will depend on the individual speeds of the trains, which determine whether some kinetic energy will remain in the center of mass of the two consists, and whether or not there is override. Nevertheless, the above results indicate that useful comparative evaluations of the various crashworthiness concepts can be obtained by including only the locomotives in the crash scenarios to be discussed below.

3.2.2.2 The Effect of Lateral Buckling

The effects of lateral and vertical buckling on the crushing response of the lead locomotive were also studied using a simplified multi-vehicle collision model. A train consisting of ten 200-ton vehicles was modeled with linear spring connections along the axis of original motion but with no rotational restraint in the horizontal plane at the connections (figure 3-6).

Lateral buckling was modeled by imposing an initial lateral displacement at one of the vehicle-to-vehicle connections. Such an approach should yield a conservative result with respect to the lead locomotive crush since, in reality, some crush would occur prior to buckling and derailment.

Figure 3-6 shows the results for the case in which the initial lateral displacement was imposed between the fifth and sixth vehicles. The implication of these results is that large lateral displacements are required before there is a significant change in the amount of energy dissipated in the lead locomotive. Since a similar result would be obtained for vertical displacement \em\ except for some small effect of gravity - we conclude that it is not necessary to include the effects of buckling or derailment of trailing vehicles in determining the crush response of the lead locomotive.

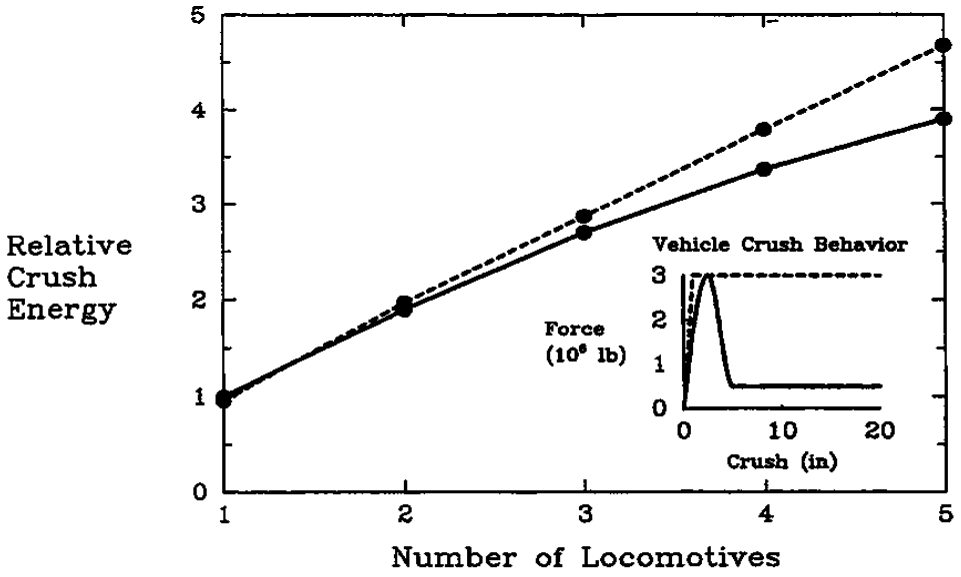

Figure 3-4. Collision Energy Dissipated in the Lead Locomotive as a Function of the Number of Trailing Locomotives of Equal Weight and Strength

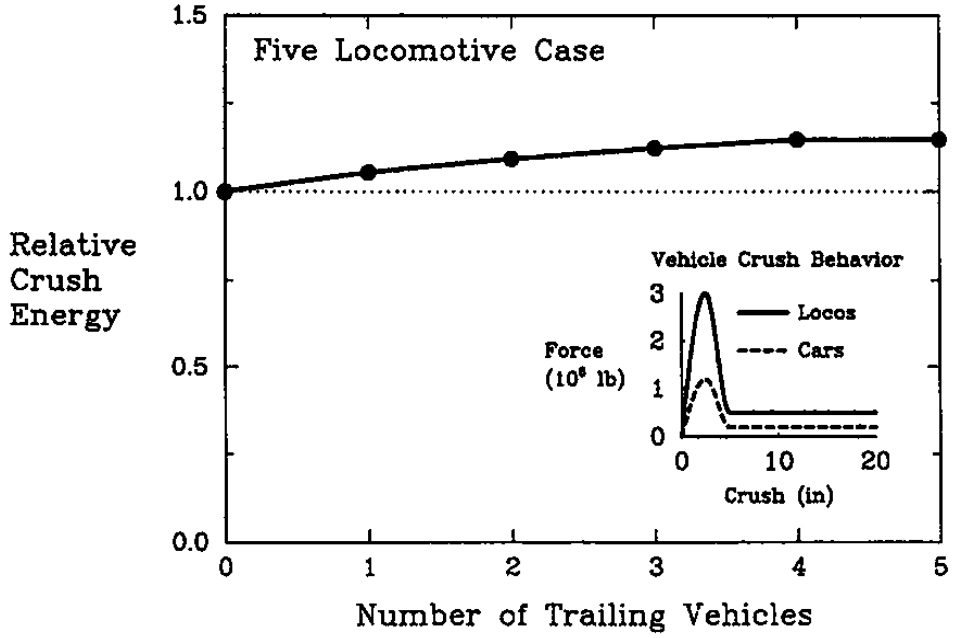

Figure 3-5. Collision Energy Dissipated in the Lead Locomotive as a Function of the Number of Trailing Vehicles of Lower Weight and Strength

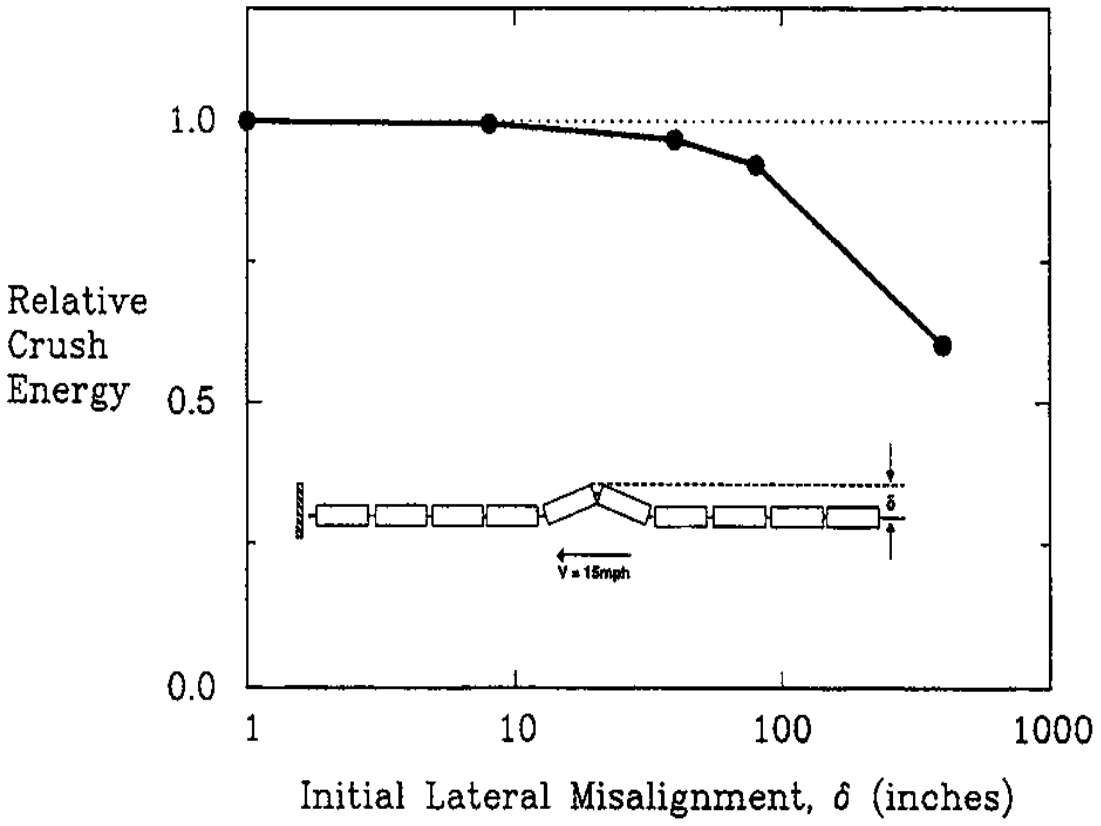

Figure 3-6. Collision Energy Dissipated in the Lead Locomotive as a Function of Lateral Displacement for a Coupler Connection

3.3 STRUCTURAL DAMAGE MODEL

The purpose of the structural damage model is to provide the load-crush curves for use in the collision dynamics calculations. These are derived from finite element analyses on component geometries derived from manufacturers' drawings for those components that participate in the collision (see section 2.2). Development of the load-crush curves was an iterative process in which results from preliminary collision dynamics calculations were used to refine the modes, locations, and extents of crushing. The refined load-crush responses are reported here.

3.3.1 General Approach

Selection of component geometries, materials, and boundary conditions formed the first part in the analysis of structural damage. There are several locomotive models on the road today that not only satisfy but generally exceed the S-580 specification and each has some unique front-end component geometry. Our approach to obtaining a single load-crush curve for each component that just satisfied S-580 (i.e., with no margin of extra strength) was to generate scaled-down components from mechanical drawings provided to us by locomotive manufacturers for current models. The scaling down process involved either decreasing plate thicknesses or lowering material strengths until the structure just satisfied S-580. Load-crush curves for components not covered by S-580, such as the draft gear support structure and the underframe, were derived from drawings of actual components and an understanding of the design constraints placed on these components.

The finite element analyses were carried out using the commercially available program ABAQUS, version 5.3. ABAQUS is recognized for its capabilities in the areas of nonlinear deformation and contact problems [4]. It accounts for several of the types of deformation anticipated during crushing of the components, including plastic deformation and collapse, and elastic and plastic buckling.

Finite element meshes for the various components were generated primarily using shell elements. Welded junctions were simulated through rigid nodal connections and the loading was in most cases applied through the controlled displacement of a contacting rigid surface. All analyses were performed under quasi-static loading conditions.

The multilinear stress-strain curve used in these analyses, shown in figure 3-7, corresponds approximately to A572 structural steel with an elastic modulus equal to 28×10^6 lbf/in^2, a yield strength at 0.2% strain of 50×10^6 lbf/in^2, and a tensile strength at 20% strain of 70×10^3 lbf/in^2, after which the strength remains constant. Strain rate effects were not included in our analyses for several reasons. While elevated strain rates increase the effective flow stress of steels, there can also be a decrease in ductility; the combined effect is difficult to establish accurately. We also felt that the effects of strain rate are small in comparison to train mass and speed. Finally, the strength values specified by S-580, which was our baseline, do not account for rate effects.

The load-crush response of the various components was reviewed to determine the extent to which load-carrying capacity would be limited by material fracture. This was accomplished

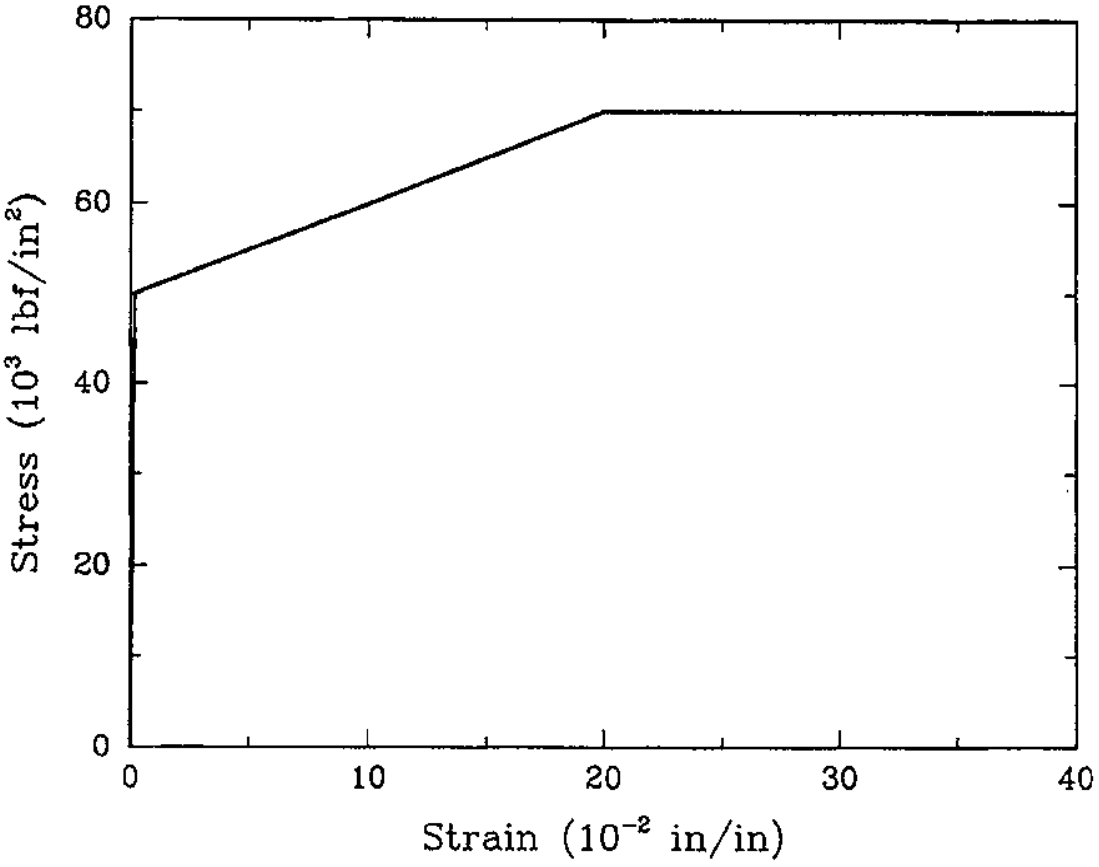

Figure 3-7. Generic Stress-Strain Curve Used in the Structural Damage Calculations

by examining maximum material strains and weld strengths, where applicable. However, for all components analyzed, the load-crush curve was not greatly affected by fracture. Therefore, the elastic-plastic deformation curves generated by finite element analysis were used for all dynamics calculations.

3.3.2 Component Analysis

3.3.2.1 Anticlimber

The finite element mesh for the baseline anticlimber is shown in figure 3-8. Nodes along the back end of the anticlimber were fixed to approximate the constraint provided by the stiff box structure of the underframe. The load-deformation response of the anticlimber corresponding to a vertical load is shown in figure 3-9. The vertical load was applied at the front edge of the anticlimber, uniformly distributed between the two gusset plates at the main underframe webs as required by S-580. This anticlimber just satisfies the 200,000 lbf strength requirement.

The calculated longitudinal load-crush curve for this component is shown as the solid curve in figure 3-10. The load in this case is applied through motion of a planar rigid surface oriented transversely to the longitudinal axis. The irregular shape of the load-deflection curve is the result of a sequence of events wherein pairs of reinforcing gusset plates build up a compressive load and then fail due to plastic buckling. The up-and-down nature of the calculated curve arises because the gusset plates are staggered in the longitudinal direction. As the rigid surface begins to crush the anticlimber, the pair of plates closest to its midplane carry most of the load in compression. As the load in these plates reaches the plastic limit, the plates fail, and the load is transferred to the next-innermost pair of plates. This pattern of loading continues until all of the gusset plates have buckled. Although the analysis was not carried out beyond about 8 inches for this case - due to numerical difficulties - we expect the load to drop with further deformation until the crushed and compacting anticlimber plates transfer load directly to the underframe structure whose longitudinal strength is much greater (see below). The idealized load-crush curve, which was the anticlimber response used in the collision dynamics analyses, is shown as the dashed curve in figure 3-12, reflecting the behavior deduced from the finite element analyses of the anticlimber and underframe.

3.3.2.2 Front Plate/Draft Gear Support Structure

The mesh for the front plate/draft gear support structure is shown in figure 3-11. Nodes along the top edge of the support structure side plates were fixed to represent their attachment to a rigid underframe surface. Nodes at which the front plate is attached to the front of the underframe were also fixed. Longitudinal loading was applied through the striker plate to simulate load transfer through the horn of the compressed coupler.

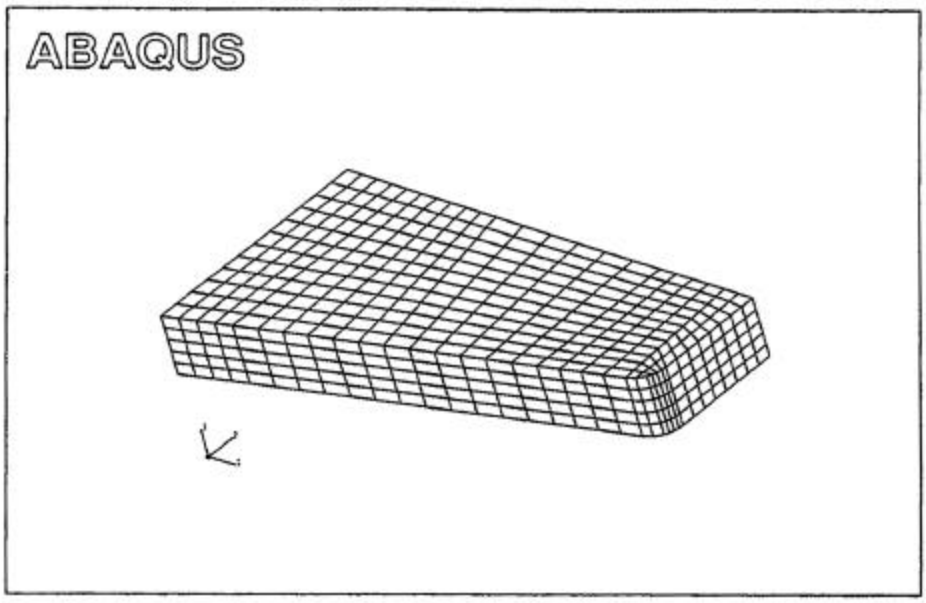

(a)

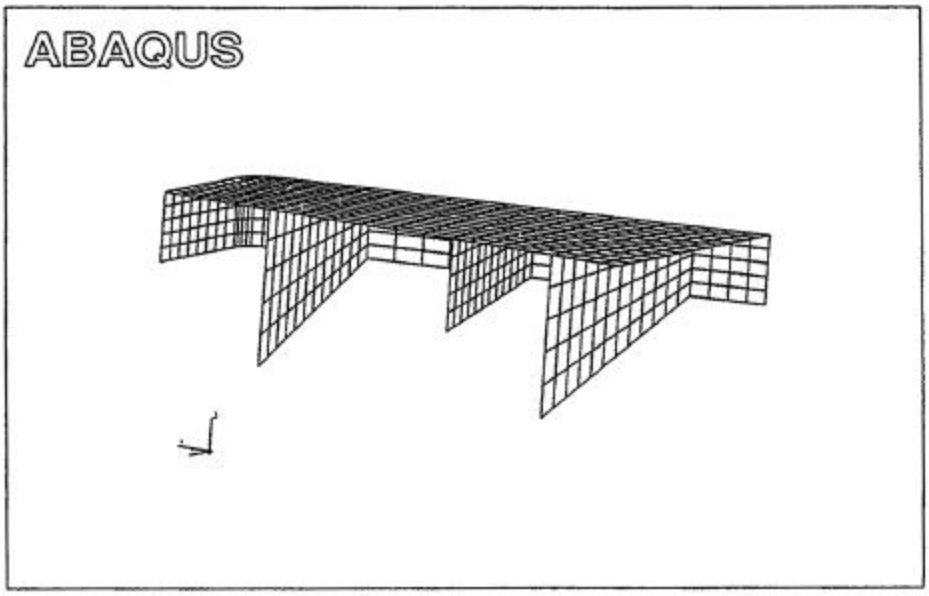

(b)

Figure 3-8. Finite Element Mesh Used in the Structural Damage Calculations of the Baseline Anticlimber (only one-half of the mesh is shown)

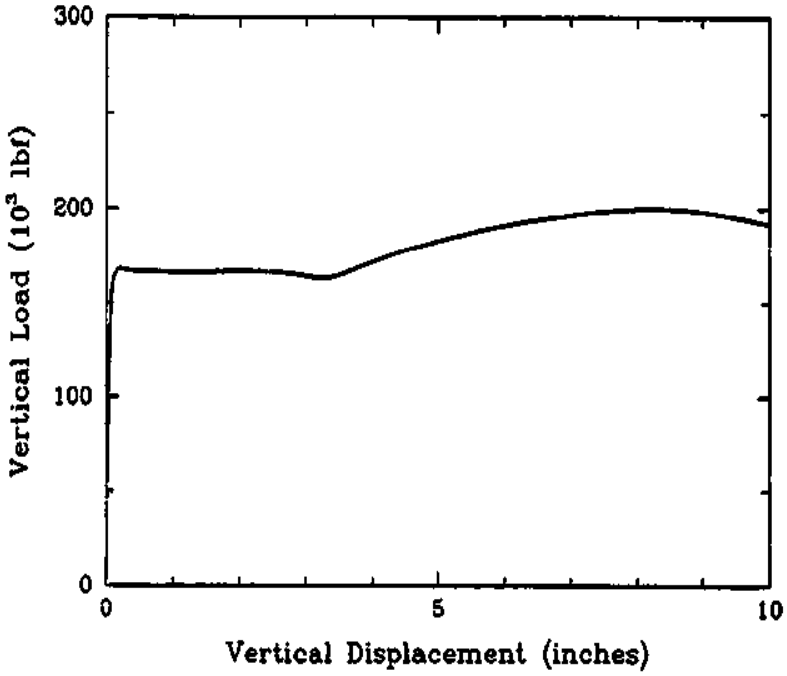

Figure 3-9. Calculated Load-Crush Curve for the Baseline Anticlimber for Vertical Loading

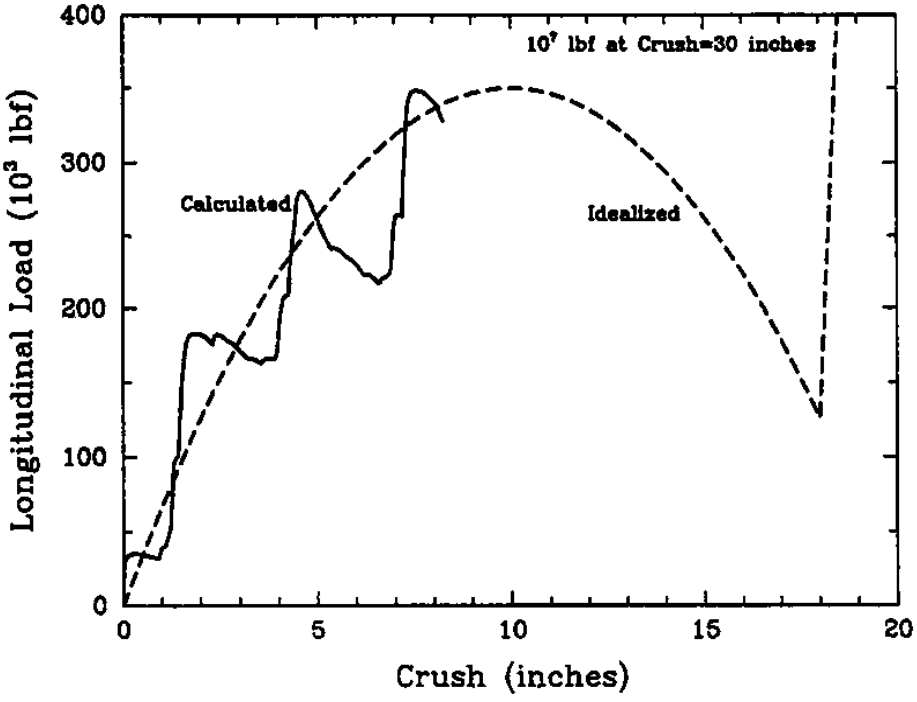

Figure 3-10. Calculated and Idealized Load-Crush Curves for the Baseline Anticlimber for Longitudinal Loading

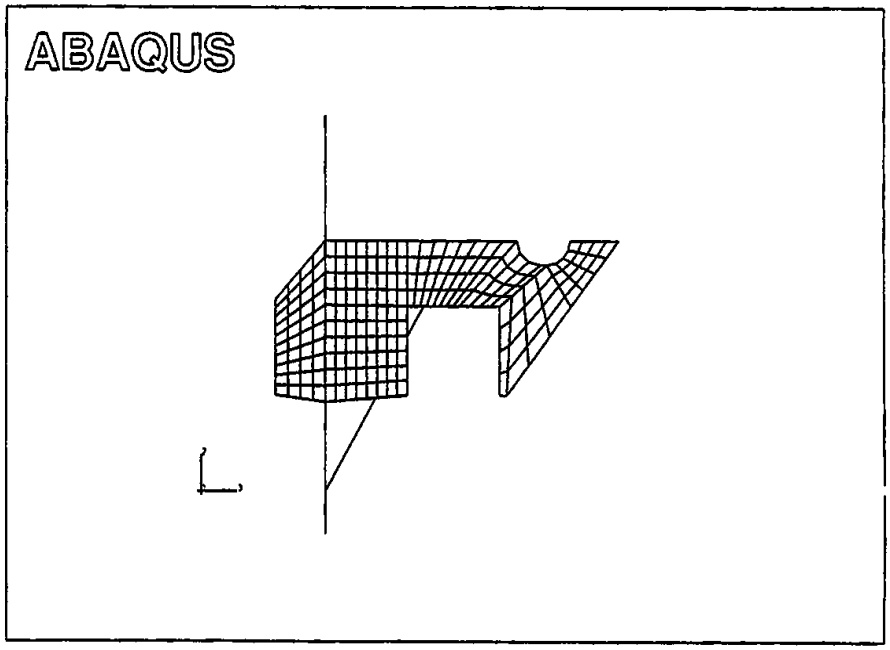

(a)

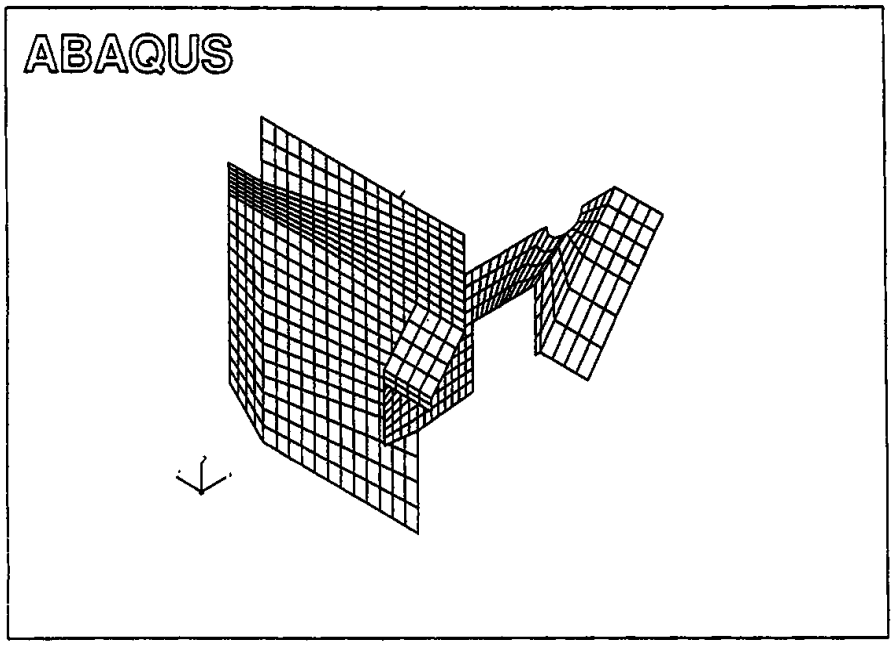

(b)

Figure 3-11. Finite Element Mesh Used in the Structural Damage Calculations of the Baseline Draft Gear Support Structure (only one-half of the mesh is shown in [b])

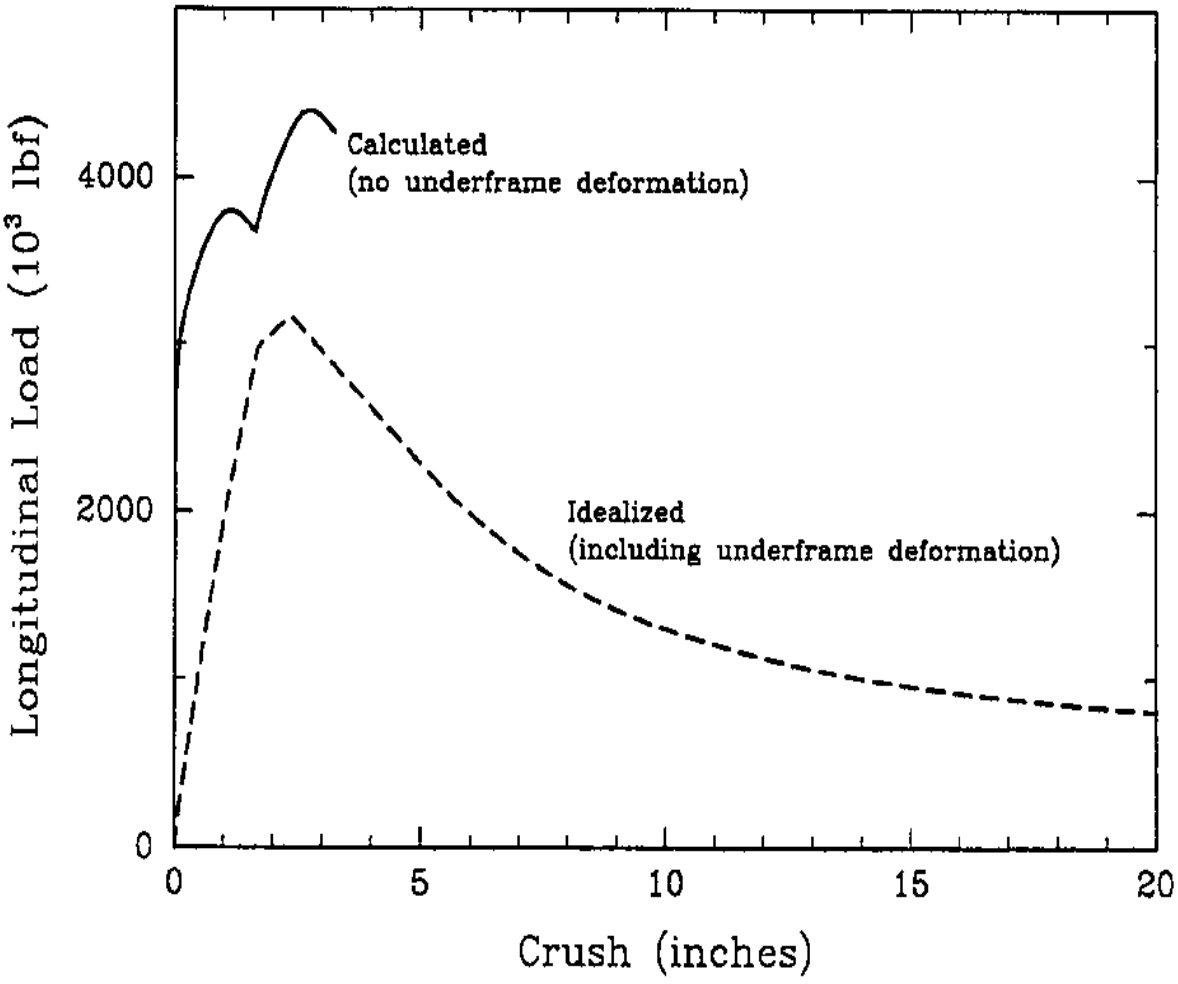

Figure 3-12. Calculated and Idealized Load-Crush Curves for the Baseline Draft Gear Support Structure for Longitudinal Loading

The computed load-crush curve of this component for crush up to four inches is shown as the solid line in figure 3-12. The analysis shows that this structure is very stiff and strong, consistent with its design requirement to withstand repeated, high buff and draft loads.

As it turns out, the draft gear support structure deformation response for a load applied to the striker plate is determined by deflection of the underframe, which is discussed below. Therefore, the underframe load-crush curve is used for the idealized draft gear support structure response, as shown by the dotted line in figure 3-12.

Analysis for fracture of this component or of bending of the underframe from the transferred load suggests that the peak striker plate load will be about 3 x 10\sub\6\sue\ lbf. Analysis for fracture indicates that failure of this component occurs when the crush at the striker plate is about one inch, which corresponds to a load of about $3x10^6$ lbf. As discussed below, our calculations also indicate that a load of this magnitude applied to the striker plate will likely initiate plastic bending in the underframe. Thus, the peak load carrying capacity applied at the striker plate is derived from two separate considerations.

3.3.2.3 Collision Posts and Short Hood Structure

A single model was used to simulate the combined action of the two collision posts and the short hood (figure 3-13) because of the S-580 specified weld attachment between these components. Figure 3-13(a) shows a side view of the short hood structure with the normally hidden collision post shaded. Figure 3-13(b) shows a view looking into the short hood from a rear vantage point; only one-half the model is shown. The combined structure was fixed at its lower edge to represent the stiff underframe. The back edge of the short hood was not constrained, in order to represent, in an approximate manner, the relatively compliant attachment of the short hood to the cab structure.

Longitudinal loading was applied through controlled motion of a convex-shaped, cylindrical, rigid surface whose axis is transverse to the longitudinal axis (figure 3-13). This surface, with a radius of 10 inches, was displaced longitudinally, contacting the front of the short hood at a height of 30 inches above the top of the sill. This location of loading, covered by S-580, is closest to that observed in head-on collisions in which override occurs (see descriptions of validation accidents below).

The load-deflection curve for the collision posts/short hood structure is shown in figure 3-14. This curve reflects the initial deformation at gradually increasing load of the front of the short hood, followed by a steep increase in the slope of the curve accompanying contact with the much stiffer collision posts. The load peaks and then drops off rapidly as the front part of the short hood collapses. Subsequently, the load remains relatively constant as the collision posts deform plastically and bend. The maximum load for deformations in which the collision posts carry the load is 400,000 lbf, or 200,000 lbf for each post, as specified in S-580.

The idealized curve used in the collision dynamics analysis is shown as the dashed curve in figure 3-14.

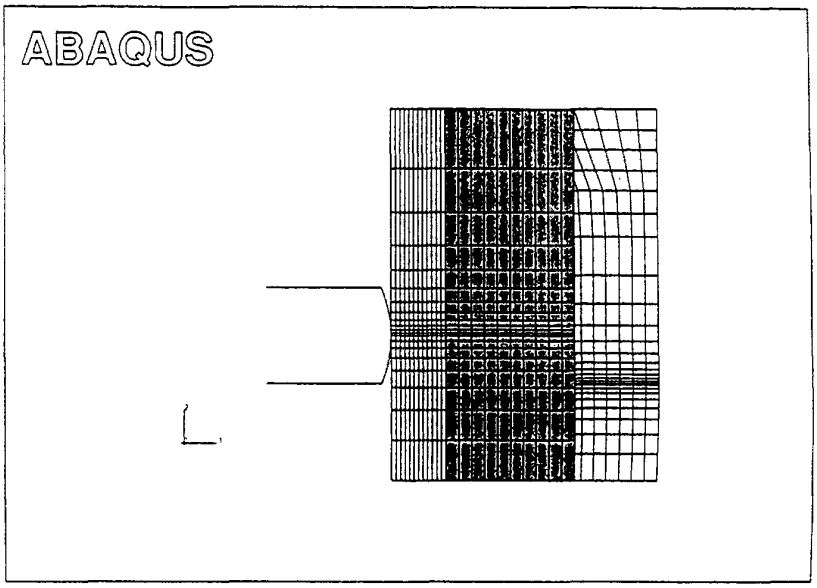

(a)

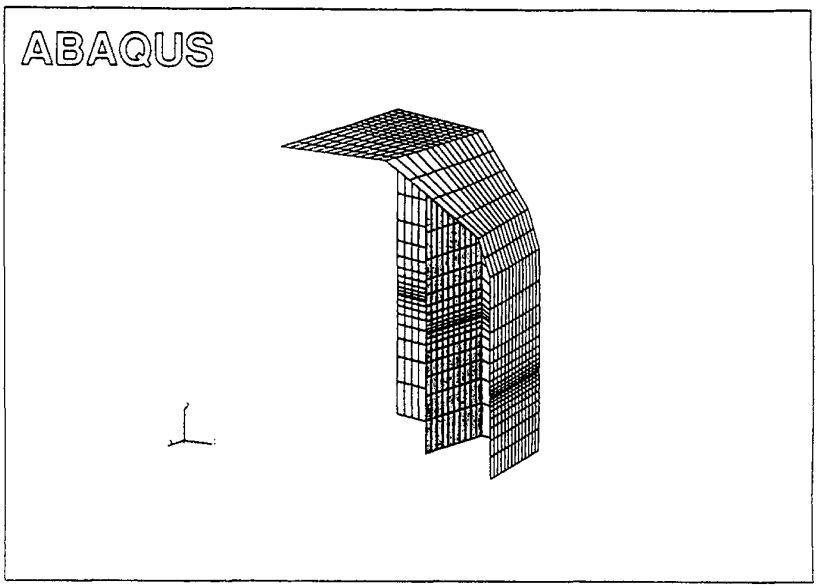

(b)

Figure 3-13. Finite Element Mesh and Loading Used in the Structural Damage Calculations of the Baseline Short Hood/Collision Post Structure (only one-half of the mesh is shown in [b])

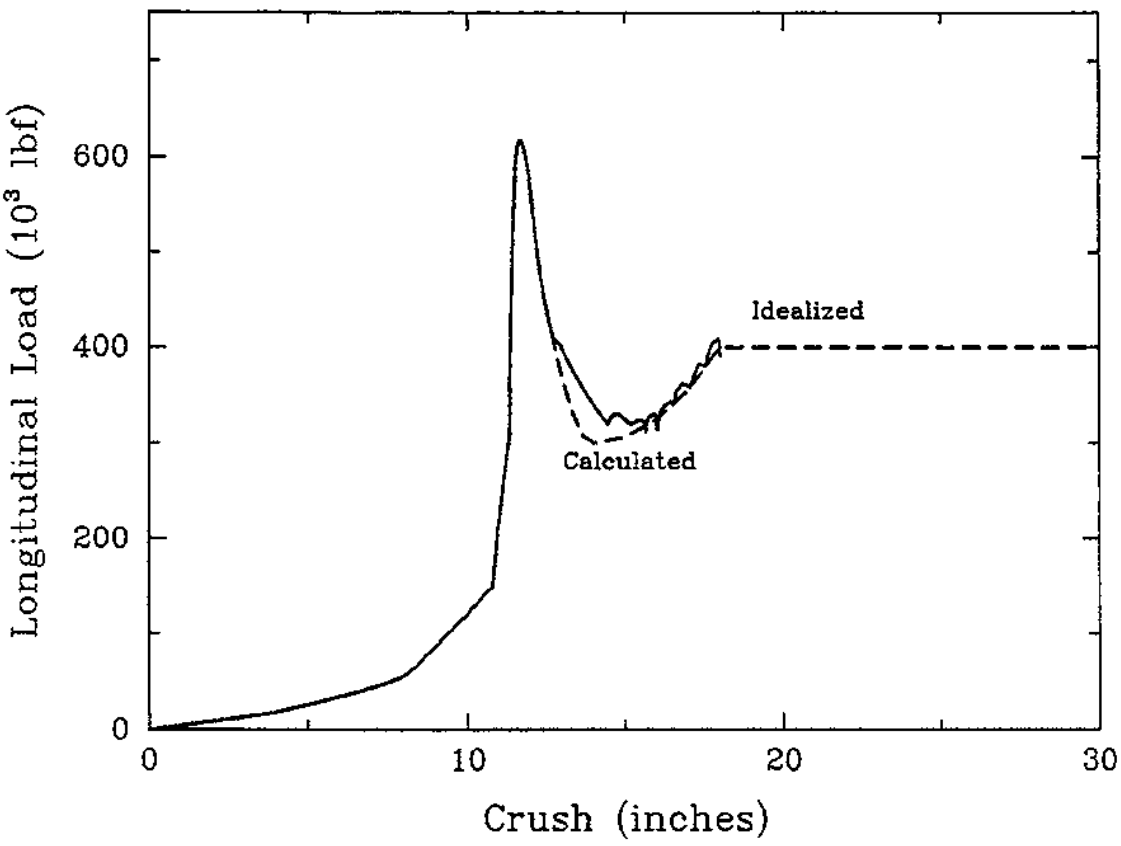

Figure 3-14. Calculated and Idealized Load-Crush Curves for the Baseline Short Hood/Collision Posts Structure for Longitudinal Loading

3.3.2.4 Underframe

Two types of underframe loading were investigated for purposes of defining load-crush curves for use in the collision dynamics calculations. In the first, an estimate was obtained of the maximum strength for a longitudinal load applied at the neutral axis of the underframe. This loading corresponds approximately to a load applied through the crushed anticlimber. The second load was applied at the level of the striker plate to obtain an estimate of the maximum bending capacity of the underframe. Underframe bending occurs when impact loads are applied at either the striker plate or at levels - such as 30 inches - above the deck of the underframe.

The underframe from the short hood end to the first bolster was modeled, as shown in figure 3-15. The mesh was constrained against vertical and longitudinal displacements and against rotation at the transverse plane that intersects the centerline of the bolster. In the first analysis, the short hood end of the mesh was loaded through a rigid, transverse plane whose displacement was specified. In the second loading, a longitudinal load was applied at the striker plate. The side plates of the draft gear support structure were modeled to provide a convenient means of applying the loads.

The load-deflection curves for the two types of loads are shown in figure 3-16. The curves indicate that the underframe modeled can support a pure longitudinal load of about 10×10^6 lbf and a bending load at the striker plate of 3×10^6 lbf. Bending of the underframe causes the load to drop markedly with increasing crush due to the increase in moment arm.

The results of these calculations were used to derive idealized load-crush curves for the anticlimber/underframe structure and the front plate/draft gear support structure, as discussed above. That is, the load for the anticlimber rises sharply to 10×10^6 lbf after substantial crush, reflecting complete load transfer to the underframe (figure 3-10). Also, the load for the front plate/draft gear support structure drops sharply after the peak load of 3×10^6 lbf is reached (figure 3-12).

One of the implications of the above calculations is that there is a maximum useful ultimate load for the collision posts dictated by plastic bending of the underframe. For the underframe geometry and material strength modeled here, that load is about 3×10^6 lbf for both posts, or 1.5×10^6 million lbf for each post, at a height of 30 inches above the deck. Other constraints, such as underframe connection strength, may provide other practical limitations to maximum collision post strength.

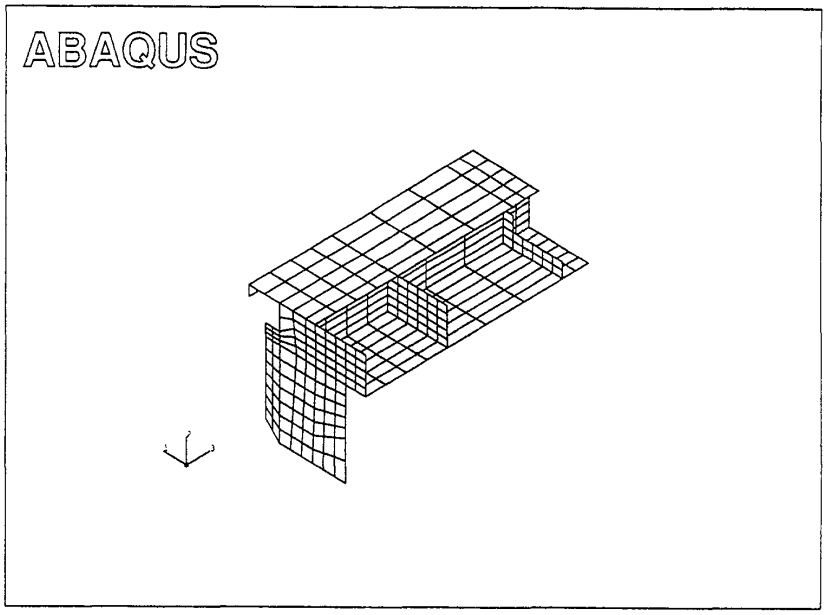

Figure 3-15. Finite Element Mesh and Loading Used in the Structural Damage Calculations of the Underframe (only one-half of the mesh is shown)

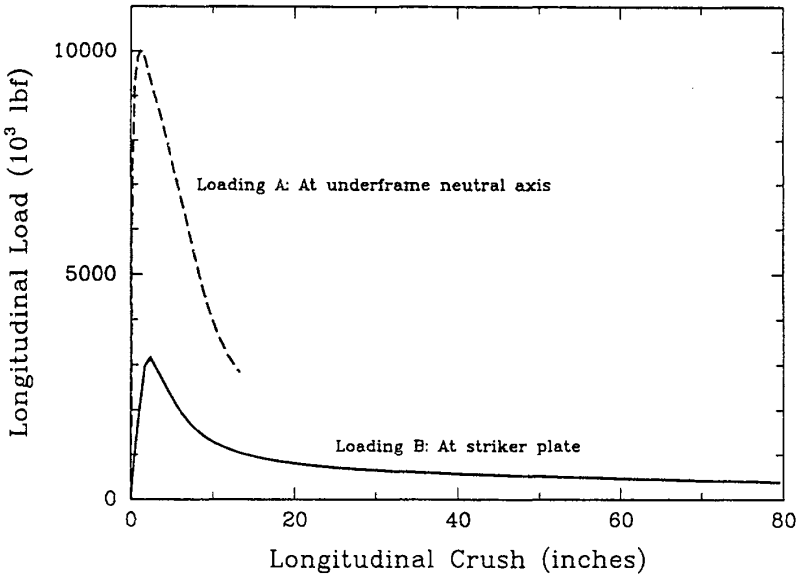

Figure 3-16. Calculated Load-Crush Curves for the Baseline Underframe for Two Types of Longitudinal Loading

4. MODEL VALIDATION

Model validation was accomplished through comparison to three head-on collisions reported in FRA accident reports. Figures 4-1 through 4-3 provide a summary of the available data on these accidents. In some cases, photographs of the final configuration of the lead locomotives were available and these are provided with the descriptions of the individual accidents.

The collision dynamics model calculations were carried out following the guidelines discussed in section 3; that is, only the locomotives were modeled, override was purposely initiated, and the lower energy absorbing override sequence was followed. Actual front end component strengths were calculated to the extent possible for the lead locomotives and actual weights were used for all locomotives in these validation calculations. Extent of longitudinal crush and crash pulse for the overridden locomotives were computed.

4.1 ACCIDENT A: LOW SPEED HEAD-ON COLLISION

This first accident, with FRA report number C-58-91, occurred between a stationary train and one moving at a speed of 18 mph, for a closing speed of 18 mph (figure 4-1). The stationary consist had three locomotives and the moving consist had only one. None of the locomotives satisfied S-580. The result of the collision, for which there are no photos, was only minor damage to the front end components. There was no override and no injuries.

The results from the ADAMS model are similar to the observations for this accident. Figure 4-4 shows the geometric interaction view of the two lead locomotives at the time of maximum crush, which was less than one inch in the draft gear support structure. (Refer to figure 3-3 for a definition of components in this view.) The crash pulse corresponding to this collision is shown in figure 4-5; the peak acceleration is eight g's.

4.2 ACCIDENT B: MEDIUM SPEED HEAD-ON COLLISION

The second accident, B-02-93, corresponds to the head-on collision of two trains, one with two locomotives traveling at 9 mph and the other with five locomotives traveling at 21 mph for a closing speed of 30 mph (figure 4-2). Again, none of the locomotives satisfied S-580. However, our structural damage calculations indicate that the collision post strength of the overridden locomotive, a GP-60 built in early 1990, was approximately 200,000 lbf per post at a height of 30 inches. On the other hand, the anticlimber on the overridden locomotive did not span the entire width of the short hood. Rather, it consisted of two triangular box sections, each centered at the main underframe webs with an open space of about 50 inches between their inner edges.

The collision resulted in override of the lead locomotive in the 9 mph train onto the lead locomotive of the other train causing substantial crush to the cabin and an occupant fatality.

Accident A: C-58-91 Head On Collission

Date: 4/21/91

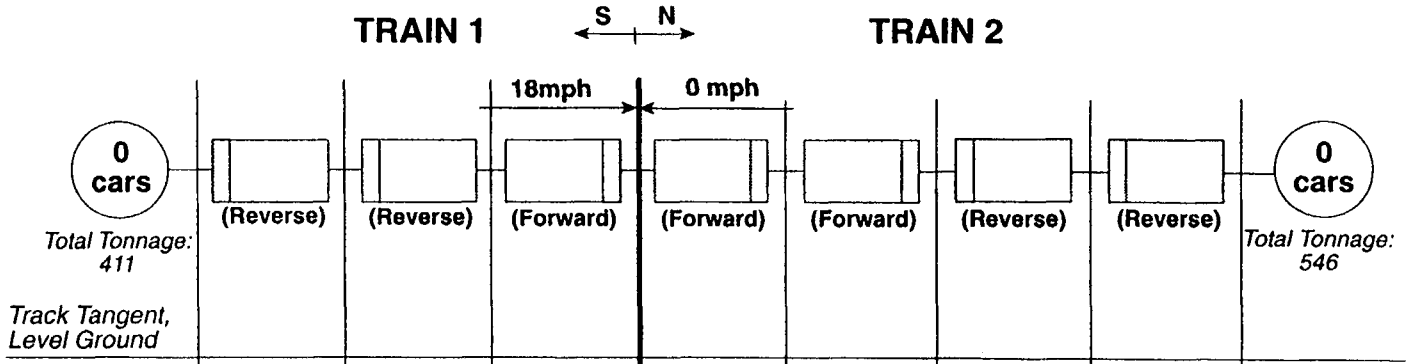

Locomotive #	CSXT-5863	CSXT-5883	CSXT-5816	CSXT-5723	CSXT-5898	CSXT-5878	CSXT-6134	
Make	B-36-7	B-36-7	B-36-7	U-36-B	B-36-7	B-36-7	SD-40-2	
Manufacture	GE	GE	GE	GE	GE	GE	EMD	
S-580	N	N	N	N	N	N	N	
Year Built	1985	1985	1985	1970	1985	1985	1975	
Length (ft)	62.2	62.2	62.2	60.2	62.2	62.2	68.8	
Weight (Tons)	140	140	140	139	140	140	184	
# of Occupants	0	0	0	0	0	0	0	
Injuries	0	0	0	0	0	0	0	
Fatalities	0	0	0	0	0	0	0	

Figure 4-1. Data Available and Derived for Crash Scenario A: Low Speed Head-On Collision with 18 mph Closing Speed

Accident B: B-02-93

Date: 1/20/93

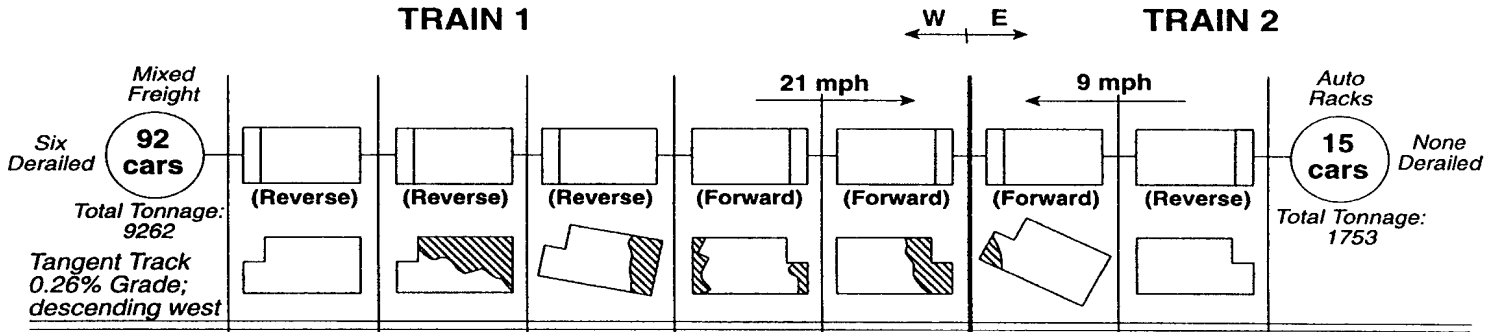

Locomotive #	SP-9346	SP-9287	CSX-6077	CSX-844	SSW-9710	BN-7072	BN-7180
Make	SD45T-2	SD45T-2	GP40-2	SD40-2	GP-60	SD40-2	SD40-2
Manufacture	EMD	EMD	EMD	EMD	EMD	EMD	EMD
S-580	N	N	N	N	N	N	N
Year Built	1975	1973	1972	1990	1990	1978	1979
Length (ft)	70.7	70.7	59.2	68.8	59.8	68.8	68.8
Weight (Tons)	205	205	139	195	143	208	208
# of Occupants	0	0	0	0	?	0	0
Injuries	0	0	0	0	?	0	0
Fatalities	0	0	0	0	1	0	0

Notes: O.R. = Override
Shaded areas correspond to regions of crush

Figure 4-2. Data Available and Derived for Crash Scenario B: Medium Speed Head-On Collision with 30 mph Closing Speed

Accident C: C-10-94

Date: 2/10/91

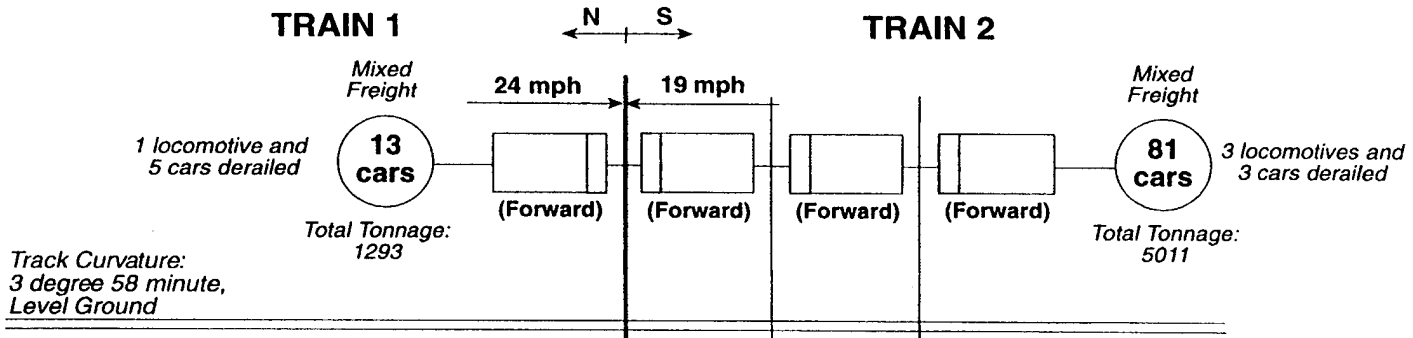

Locomotive #	KCS 705	KCS 741	KCS 721	KCS 677
Make	SD 50	SD 60	SD 60	SD 40-2
Manufacture	EMD	EMD	EMD	EMD
S-580	N	Y	N	N
Year Built	1981	1991	1989	1978
Length (ft)	71.2	71.2	71.2	68.8
Weight (Tons)	184	184	184	184
# of Occupants	3	2	0	0
Injuries	3	2	–	–
Fatalities	0	0	0	0

Figure 4-3. Data Available and Derived for Crash Scenario C: Medium Speed Head-On Collision with 43 mph Closing Speed

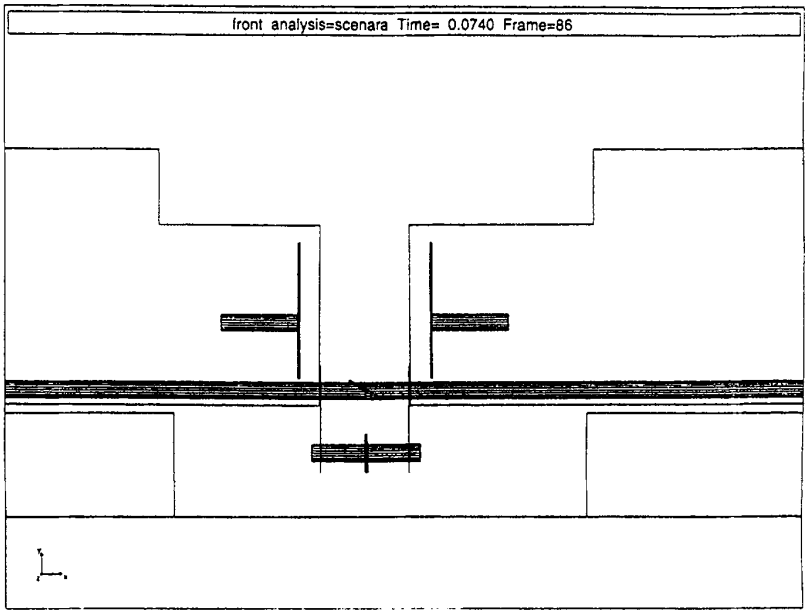

Figure 4-4. ADAMS View of the Front End Interaction at the Point of Maximum Lead Locomotive Crush for Scenario A, 18 mph Closing Speed

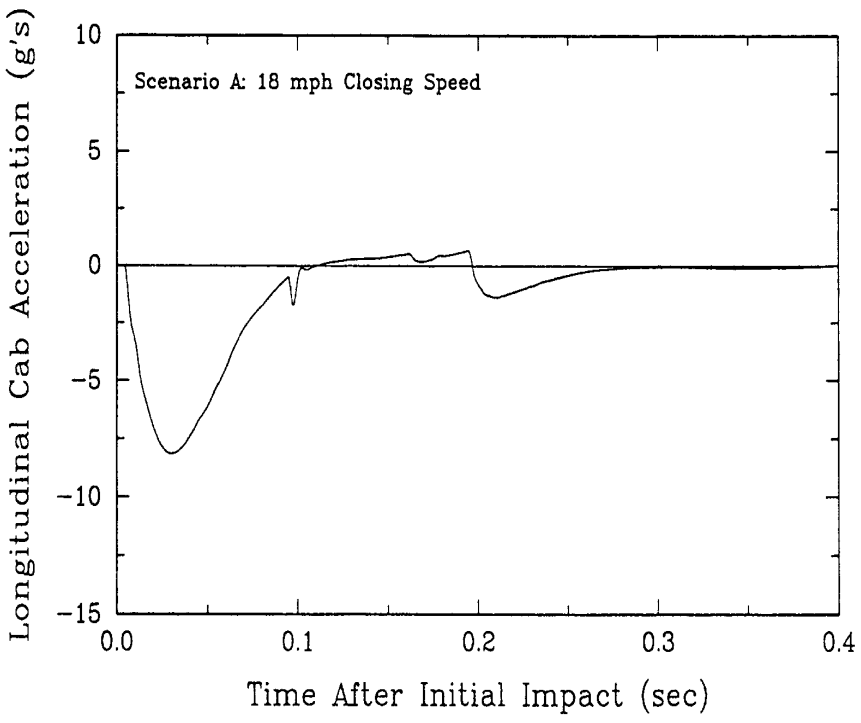

Figure 4-5. Lead Locomotive Crash Pulse Predicted for Scenario A, 18 mph Closing Speed

Figure 4-6 is a photo of the configuration of the lead locomotives after the collision. The sill heights of the two locomotives were within one inch of each other.

Again, the ADAMS calculation results agree with the observations of this accident. Figure 4-7 shows the front end interaction view from ADAMS for the point of maximum lead locomotive crush. Override is predicted as is substantial crush of the short hood structure and the cab (note position of short hood/collision post impact element in the left locomotive). The model does predict about 10 ft of crush beyond the tip of the short hood compared to what appears to be about 7-8 ft from the photo. Figure 4-8 shows the overridden cab acceleration vs. time. The peak acceleration in this accident is just over 10 g's and is due to loading of the stiff draft gear support structure/underframe.

Figure 4-9 shows a side view photograph of the overriding locomotive in this accident, after the two lead locomotives have been pulled apart. This photo suggests that very little of the draft gear support structure remains, which is consistent with the lower energy override sequence used in the model and as discussed in section 2.3. Figure 4-10 shows a front view of the overridden locomotive, again after the two locomotives have been pulled apart. The coupler is intact, even though there is a large indentation in the striker plate indicating that the coupler sustained a high longitudinal load. Also noteworthy from this photo is the amount of shear experienced by the front end as the opposing locomotive overrode.

Although the lead, overridden locomotive in this accident did not satisfy S-580, our analysis suggests that total override would have occurred and that crush, though somewhat less, would still have eliminated the survivable cab space. Consequently, the locomotive configuration and initial train speeds for this particular accident were selected as the baseline crash scenario for use in evaluating the design concepts to be generated later in this program and reported in volume 2.

4.3 ACCIDENT C: MEDIUM SPEED HEAD-ON COLLISION

The third accident modeled, FRA number C-10-94, was for a single locomotive consist traveling at a speed of 25 mph colliding head-on with a three locomotive consist traveling at 18 mph for a closing speed of 43 mph (figure 4-3). The lead locomotive of the 18 mph consist, which was built in early 1991 and satisfied S-580, was overridden but the collision posts were effective in arresting the override. There were only minor injuries. Figure 4-11 shows a photo of the front of the overridden locomotive after the two locomotives were pulled apart. It appears that the short hood has been crushed about two feet.

The collision dynamics model results for this accident were in general agreement with the observations. The overridden locomotive contained collision posts whose calculated strengths were over 400,000 lbf each, and this greater strength was included in the model. Figure 4-12 shows the lead locomotive interaction view at the point of maximum crush. Override is predicted to occur and the predicted crush of the short hood/collision post structure is about 4.5 feet. Figure 4-13 shows the crash pulses predicted for this accident.

Again, examination of other photos for this accident suggests that the draft gear support structure of the overriding locomotive was essentially sheared off.

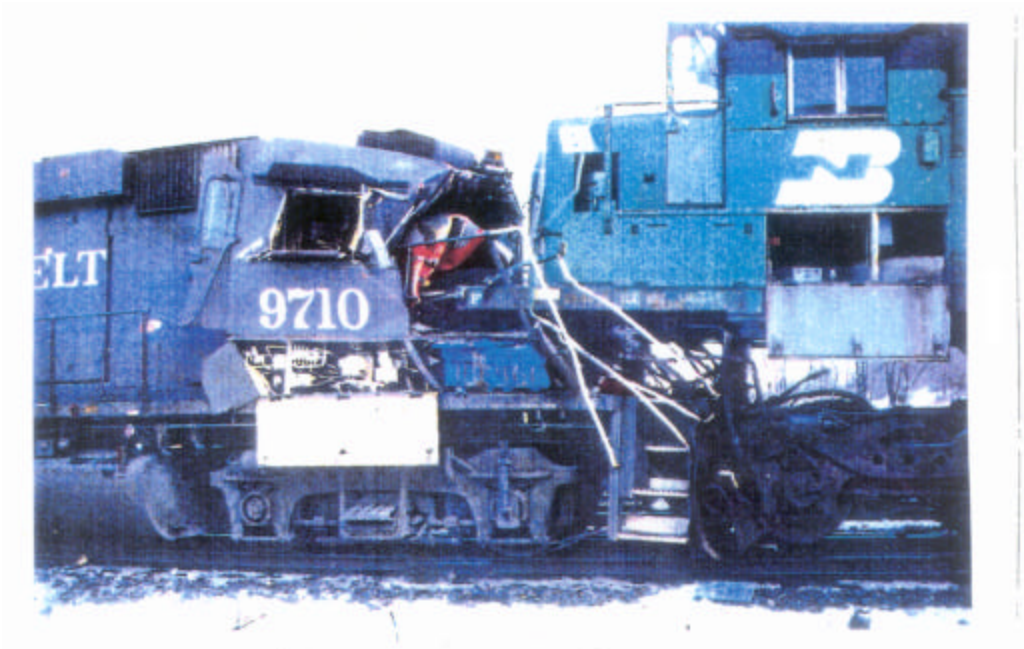

Figure 4-6. Photograph of the Override between the Two Lead Locomotives in Scenario B, 30 mph Closing Speed

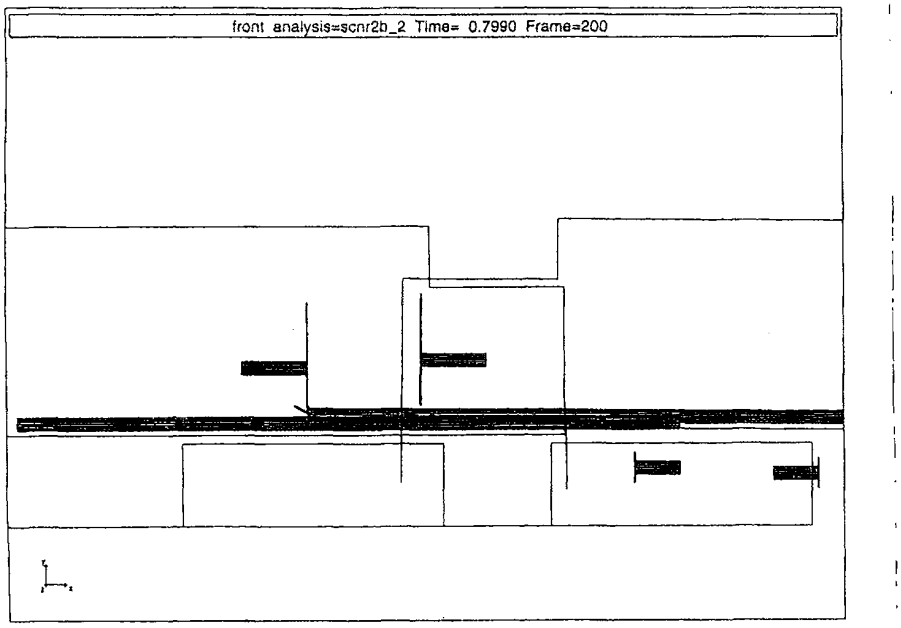

Figure 4-7. ADAMS View of the Front End Interaction at the Point of Maximum Lead Locomotive Crush for Scenario B, 30 mph Closing Speed

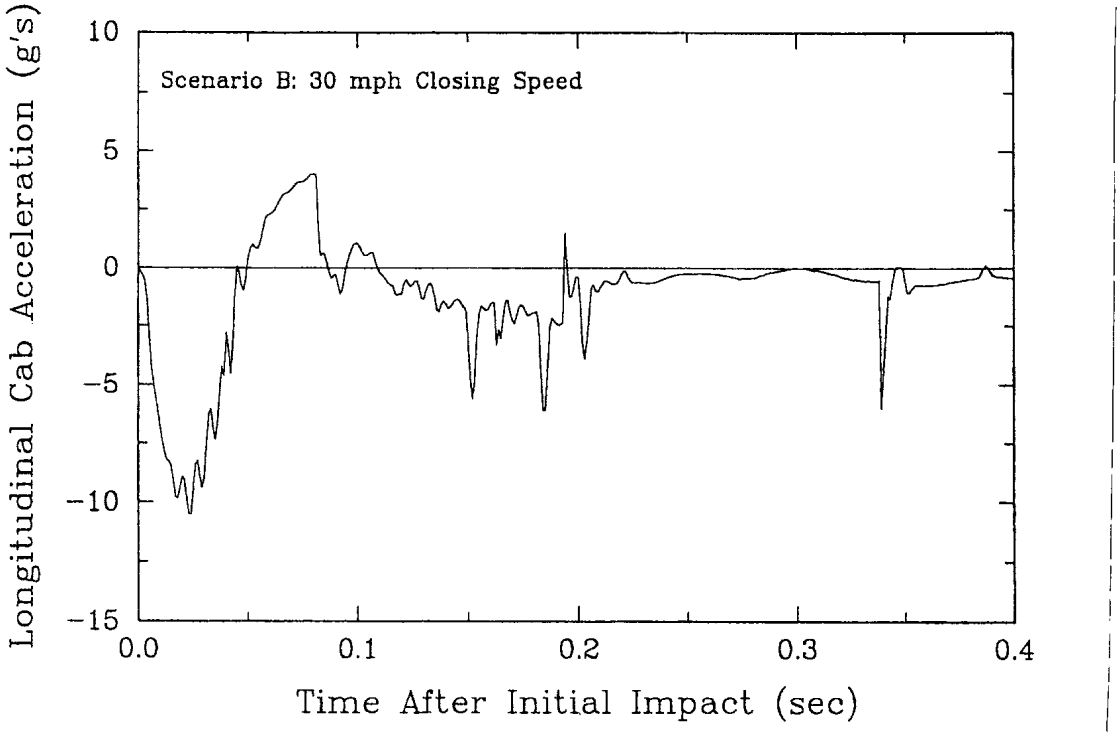

Figure 4-8. Lead Overridden Locomotive Crash Pulse Predicted for Scenario B, 30 mph Closing Speed

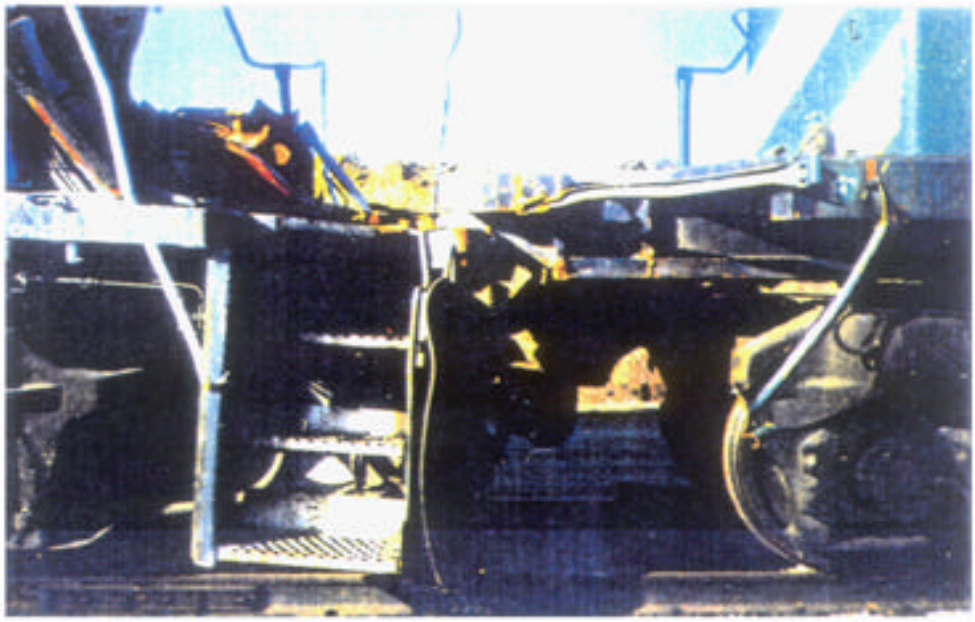

Figure 4-9. Side View Photograph of the Overriding Lead Locomotive Front End in Scenario B, after Being Pulled from the Overridden Locomotive, Showing the Damage to the Draft Gear Support Structure

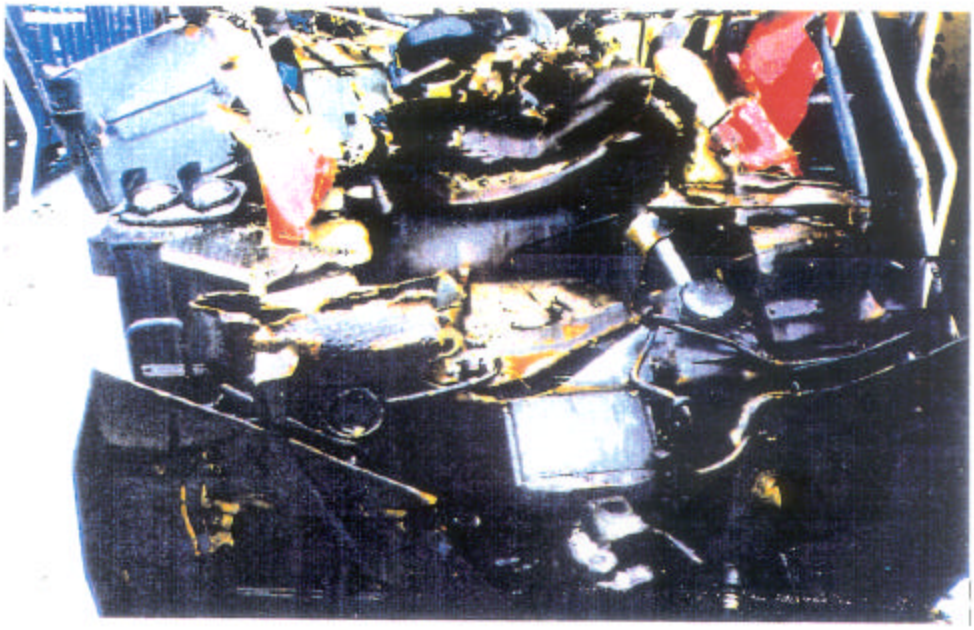

Figure 4-10. Front View Photograph of the Overridden Lead Locomotive in Scenario B, Showing Extensive Shearing of Components

Figure 4-11. Front View Photograph of the Overridden Lead Locomotive in Scenario C, Showing the Limited Short Hood Structure Crush

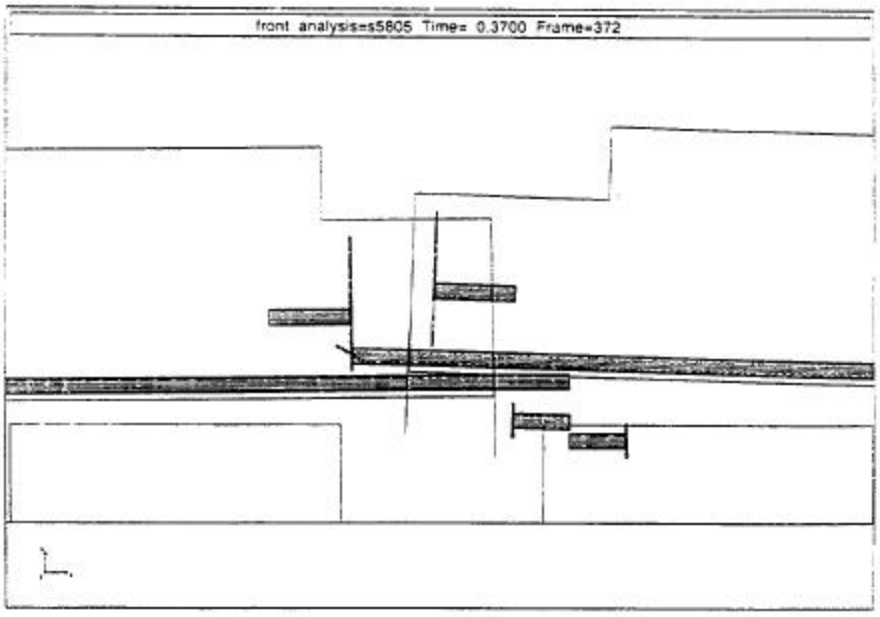

Figure 4-12. ADAMS View of the Front End Interaction at the Point of Maximum Lead Locomotive Crush for Scenario C, 43 mph Closing Speed

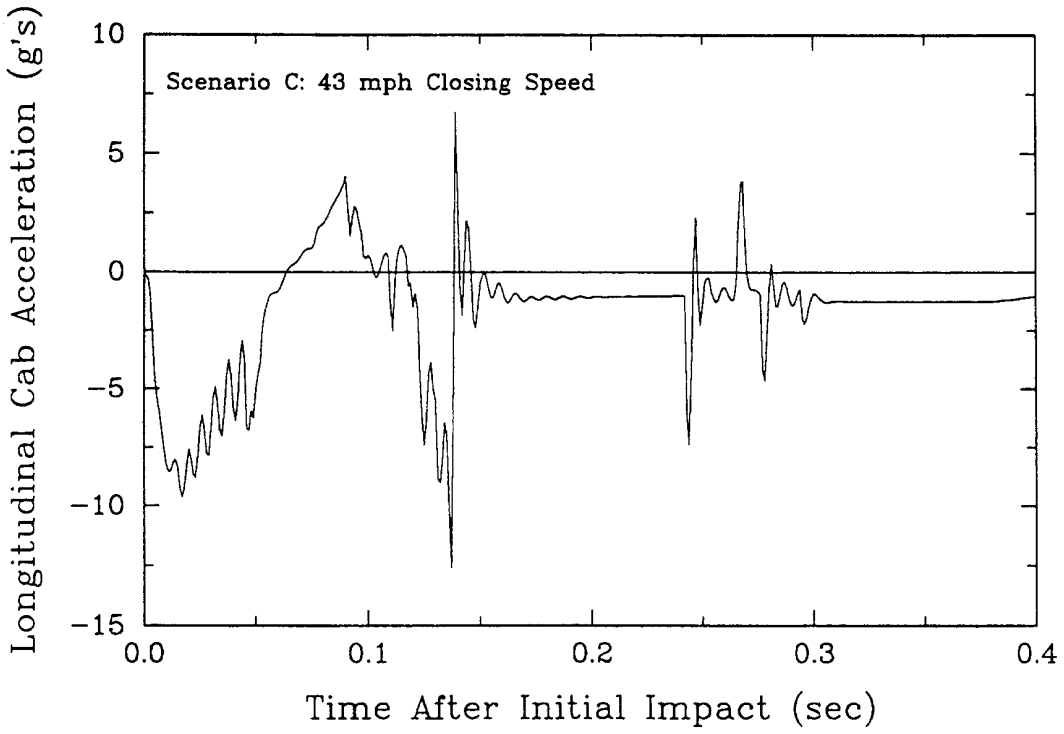

Figure 4-13. Lead Overridden Locomotive Crash Pulse Predicted for Scenario C, 43 mph Closing Speed

5. CONCLUSIONS

The model developed to simulate the head-on collision of two lead locomotives, each in a multi-locomotive, multi-trailing-vehicle train, appears to provide a good simulation of the resulting extent of override and crush in the lead locomotives. Results of this study show that trailing vehicles (nonlocomotives) and the effects of derailment need not be modeled to predict the crush response of the lead locomotives. Comparison of the model predictions to observations for three accidents described in FRA reports are all in good agreement. Although the model has been validated for closing speeds up to 43 mph, we believe that it can provide useful results on lead locomotive crush response for higher speeds. The model is currently limited to freight locomotives whose front end components are similar to those considered here.

The accident results and model predictions also show that override of locomotives satisfying S-580 can occur in medium speed collisions. This is apparently possible because the anticlimber of the overridden locomotive is not loaded vertically as apparently envisioned in the formulation of S-580. Rather, the deformation and failure of the draft gear support structure of the overriding locomotive, together with ramping between coupler or anticlimber components in colliding locomotives, permits a path for override to occur. The anticlimber does appear to provide benefit in preventing rising debris from reaching the cab in a grade crossing collision and in absorbing some collision energy. Also, the accident observations and model results do not rule out possible benefit from a modified anticlimber designed to assure trapping.

A particular result of the model, confirmed to some extent by one of the accidents, is that override and substantial cab crush can occur in a locomotive that satisfies S-580 in a head-on collision with a closing speed of 30 mph. This crash scenario, which involves a total of seven locomotives, will be the baseline scenario with which crashworthiness improvements over those provided by S-580 will be assessed and described in volume 2 of this report series.

APPENDIX

The result that locomotive crush can be independent of the number of trailing cars can, in part, be understood from analytical considerations. Consider a multi-vehicle consist with a locomotive exhibiting rigid-plastic crush behavior, with yield load, Fy, and trailing vehicles which exhibit rigid-plastic crush behavior with a smaller yield load, f-Fy, where f is a factor less than one. By a simple energy balance, the energy dissipated in the first locomotive is equal to its own initial kinetic energy plus the work done on the locomotive by the rest of the consist:

$$E_{diss}^{loco} = E_{kinetic}^{loco} + W_{external} \ .$$

The energy dissipated in the first locomotive is primarily the work of crushing, so that, with the postulated crush behaviors, we can substitute for the crush energy and external work terms:

$$F_y \delta_c = E_{kinetic}^{loco} + f F_y \delta_c \ ,$$

where δ_c is the crush of the locomotive. Solving for *5,* we find that the amount of crush,

$$\delta_c = \frac{E_{kinetic}^{loco}}{F_y(1-f)} \ ,$$

and therefore the amount of energy dissipated during the crush,

$$E_{diss}^{loco} = F_y \delta_c \ ,$$

is independent of the number of cars trailing the locomotive.

In subsequent numerical studies of 10-body systems, we were able to produce results for energy dissipation that were within one percent of the theoretical values, confirming that when the locomotive crush strength is greater than that of the trailing vehicles, the energy dissipated is independent of the number of cars, despite the increase in kinetic energy.

REFERENCES

1. Johnson, R. M. 1993. *Assessment of Crashworthiness of Locomotives.* Final Report to the Federal Railroad Administration, U.S. Department of Transportation, Report V06200, Contract DTFR53-82-C-00042.

2. Tong, P. 1983. Rail Vehicle Structural Crashworthiness. Chapter 14 in *Structural Crashworthiness*, edited by N. Jones and T. Wierzbicki. London: Butterworths.

3. ADAMS, Solver Reference Manual. Mechanical Dynamics, Inc., Ann Arbor, MI.

4. ABAQUS. Hibbitt, Karlsson & Sorensen, Inc., Pawtucket, RI.